

Late Paleozoic Remagnetization on the Western Slope of the Southern Urals: Age and Geotectonic Implications

M. B. Anosova^{a, *} and A. V. Latyshev^{a, b, **}

^a *Schmidt Institute of Physics of the Earth, Russian Academy of Sciences, Moscow, 123242 Russia*

^b *Faculty of Geology, Moscow State University, Moscow, 119991 Russia*

**e-mail: mai.anosova@yandex.ru*

***e-mail: anton.latyshev@gmail.com*

Received June 13, 2023; revised October 14, 2023; accepted October 16, 2023

Abstract—In the paper, we present the results of paleomagnetic studies on numerous intrusive bodies of the Bashkirian megazone, a major tectonic zone of the Southern Urals. More than 70 intrusions in various parts of the Bashkirian megazone (in the northern, central, and southern part of the structure) were sampled. The studied intrusions have Riphean age. However, as a significant part of the rocks of the Southern Urals, these intrusive bodies were remagnetized during the Late Paleozoic collision within the Urals fold belt. Here, we discuss the secondary Late Paleozoic component of natural remanent magnetization. According to the obtained paleomagnetic data, the secondary Late Paleozoic component in most of the Bashkirian megazone is post-folding, i.e., formed after the completion of the main phase of fold deformations in the Southern Urals. A comparison of paleomagnetic directions obtained from intrusions in different parts of the Bashkirian megazone showed that there were no significant movements of individual parts of the Bashkirian megazone relative to each other after the formation of the Late Paleozoic component. The Late Paleozoic remanence component yielded a paleomagnetic pole of $Plong = 171.6^\circ$, $Plat = 39.9^\circ$, $\alpha_{95} = 5.9^\circ$, and $N = 6$ from six regions (38 sites) in the Bashkirian megazone. The obtained pole is statistically indistinguishable from the mean of 15 poles for Stable Europe with ages of 280–301 Ma. Thus, the secondary Late Paleozoic component in the Bashkirian megazone formed approximately 280–301 million years ago, after which the Bashkirian megazone did not experience any relative motions with respect to the East European craton.

Keywords: paleomagnetism, Bashkirian megazone, Southern Urals, Riphean, Late Paleozoic, dike complexes, reconstruction of folding processes, remagnetization

DOI: 10.1134/S1069351324700393

INTRODUCTION

Numerous intrusive bodies of the Bashkirian megazone have been formed in the Riphean during rifting in the epicontinental basin of the East European platform (Bogdanova et al., 2008; Ernst et al., 2008; Puchkov, 2010; Ross, 2011). In the Late Paleozoic, the Bashkirian megazone was subjected to syn-collisional deformations, which led to the formation of the Ural fold system. Most of the rocks were remagnetized and acquired a metachronous (secondary) component of natural remanent magnetization (Komissarova, 1970; Danukalov et al., 1982; Shipunov, 1993). This offers a possibility of gaining new and more detailed knowledge regarding the collision processes in the Southern Urals by paleomagnetic studies of remagnetized magmatic bodies of the Bashkirian megazone. The secondary Late Paleozoic remanence component will be discussed in this paper.

GEOLOGY OF THE REGION AND OBJECTS OF STUDY

The Bashkirian megazone (BM) is a large tectonic zone of submeridional strike in the folded system of the Southern Urals. In the west, through the zone of foreland thrusts, the BM borders with the East European platform (EEP). The Bashkirian megazone borders with the Zilair megazone in the south-southeast, with the Uraltau zone in the southeast, the Magnitogorsk megazone through the Main Uralian Fault in the east, and the Ufaley zone in the northeast (according to geological maps (Kozlov et al., 2001; Knyazev et al., 2013) (Fig. 1).

The Bashkirian megazone is composed of thick strata of predominantly Riphean (1650 ± 50 – 600 ± 10 Ma (Semikhatov et al., 1991)) sedimentary and volcanic-sedimentary rocks intruded by numerous intrusive bodies (Figs. 2 and 3). Besides, in the extreme north of BM, there is the Taratash salient of crystalline rocks of the East European platform basement (Puchkov,

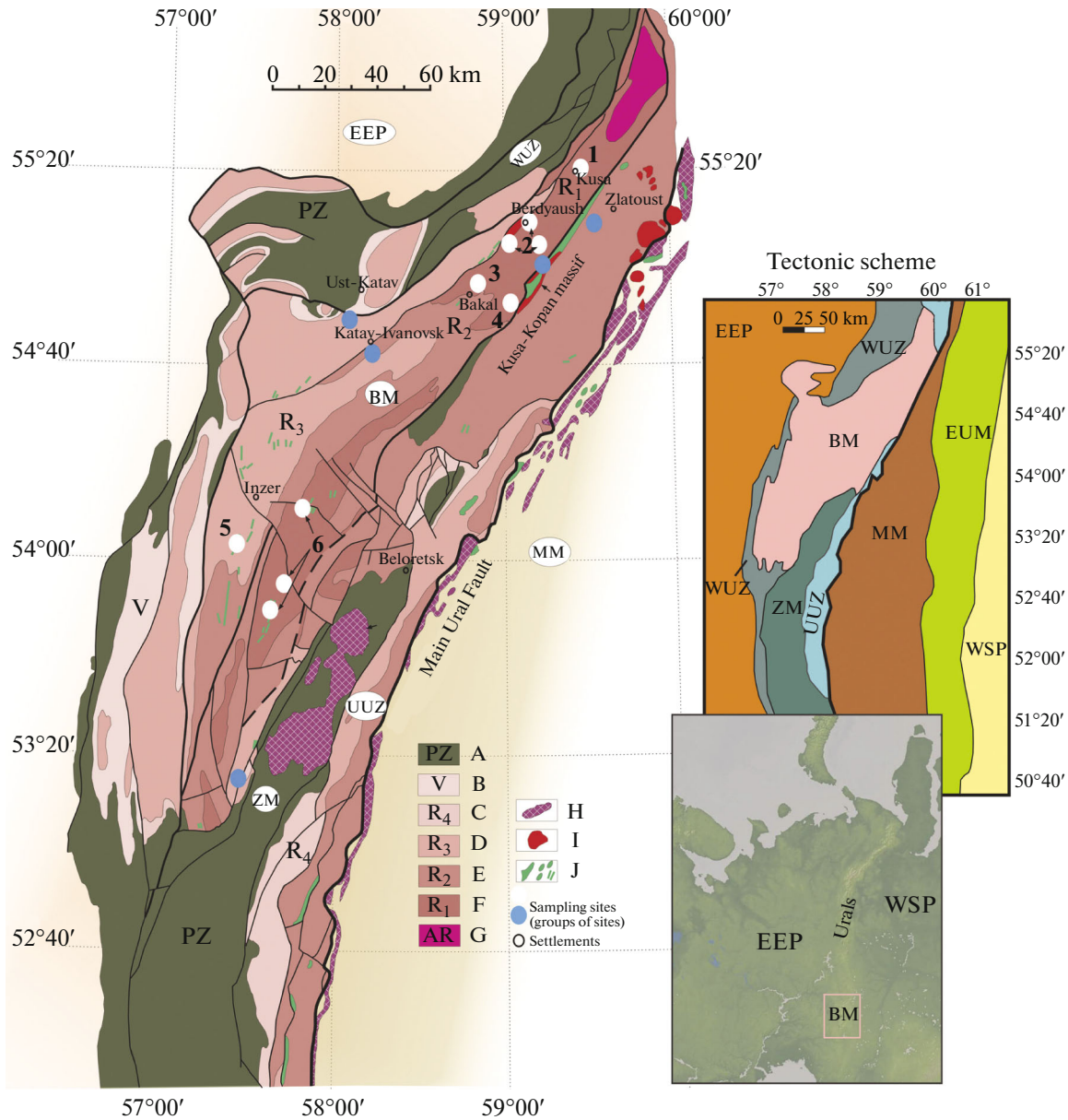


Fig. 1. Geological scheme of the South-Western Urals. Location of the Bashkirian megazone on a satellite image and in the tectonic structure of the Southern Urals. The diagrams are compiled according to the geological map and tectonic scheme in (Kozlov et al., 2001), with corrections from (Puchko, 2010), with simplifications. Tectonic units: EEP—East European platform; WUZ—Western Uralian zone of external folding, BM—Bashkirian megazone, ZM—Zilair megazone; UUZ—Uraltau-Ufaley zone (Uraltau zone in the south and Ufaley zone in the north), MM—Magnitogorsk megazone, EUM—East Uralian megazone, WSP—West Siberian plate. The letters A–J in the geological scheme indicate: A—Paleozoic undivided formations; B–F—Riphean and Vendian sedimentary deposits; G—Archean–Early Proterozoic metamorphic complexes of the basement of the East European platform. Plutonic complexes (H–J): H—ultramafic rocks of ophiolite complexes; I—felsic intrusions; J—mafic intrusions; 1–6—sampling areas (numbering corresponds to that given in the text). Sampling sites for intrusive bodies (groups of intrusive bodies) assigned to any of the areas are indicated by white circles, other sampling sites are shown by blue circles.

2010). This is one of the few places on Earth, where the geological record of Riphean is most completely and consistently preserved. Here, the Russian Riphean stratotype was identified. Stratified deposits of the Bashkirian megazone in the Upper Precambrian scale of Russia are divided into lower, middle, and upper

Groups corresponding to three large transgressive-regressive series (with age boundaries of 1650 ± 50 , 1350 ± 20 , and 1030 ± 20 , 600 ± 10 million years (Semikhatov et al., 1991)). At the beginning of the episodes, magmatism associated with rifting is noted. Some researchers also highlight the terminal Riphean

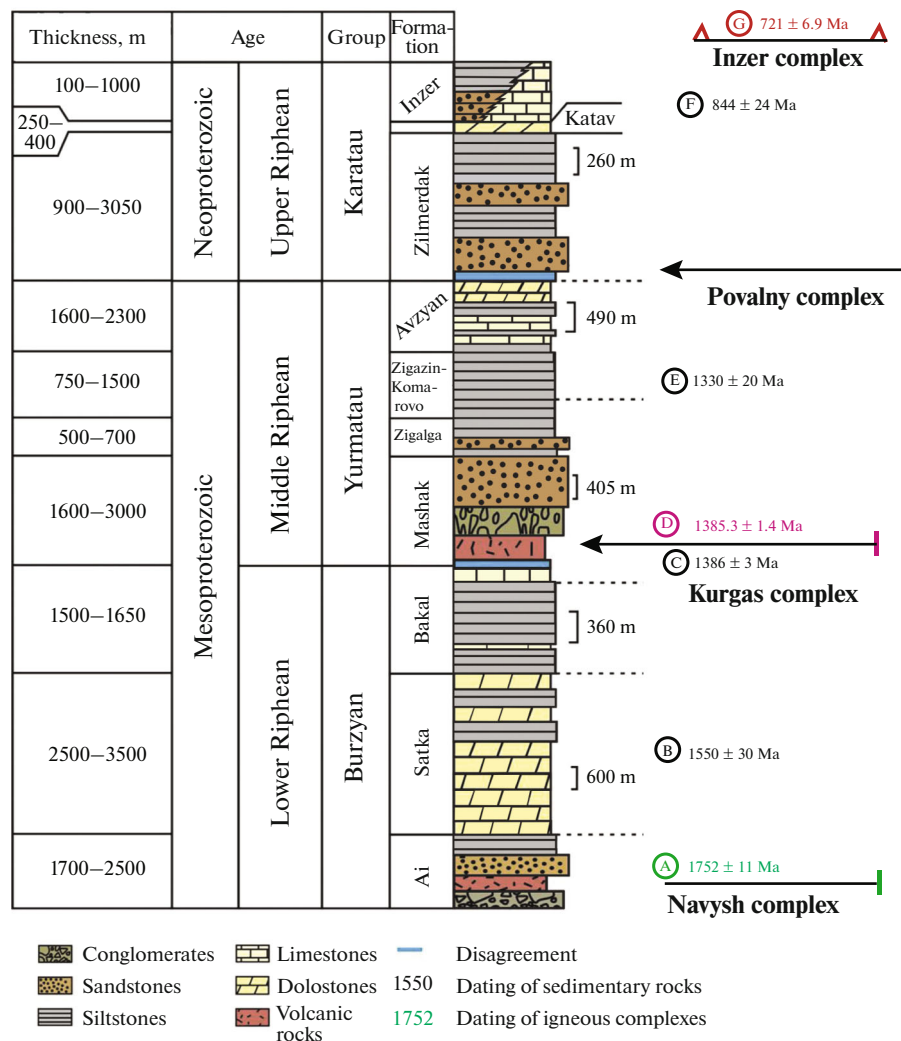


Fig. 2. Stratigraphic column of the Bashkirian megazone (Doyle et al., 2018) with additions. Igneous complexes are labeled on the right; the arrow shows the stratigraphic units with which the igneous complexes are correlated by age. Dating: A—U-Pb based on zircons (Krasnobaev et al., 2013), B—Pb—Pb age of carbonates of the Satka Formation (Kuznetsov et al., 2008), C—U-Pb based on zircons (Puchkov et al., 2013), D—U-Pb, ID TIMS, based on zircons (Ernst et al., 2006), E—Pb—Pb, phosphorite nodules of the Zigazino-Komarovo Formation (Ovchinnikova et al., 2013), F—Pb—Pb, carbonates (Kuznetsov et al., 2017), and G—U-Pb, gabbroids (Knyazev et al., 2013).

in the Southern Urals (Puchkov, 2010; Puchkov et al., 2017). In the Riphean, an epicontinental basin, which was a part of the East European platform, is believed to be developed in the territory of the Bashkirian megazone (Maslov et al., 1997; Maslov, 2004; Bogdanova et al., 2008; Puchkov et al., 2013; Kholodnov et al., 2017). Stages of rifting and related magmatism may mark the breakup of Precambrian supercontinents. For example, the Middle Riphean Mashak magmatic event at the boundary of the Early and Middle Riphean is associated with the breakup of the Nuna supercontinent (Ernst et al., 2008; Puchkov, 2010; Evans and Ross, 2011). We attribute the formation of a significant part of the studied igneous objects (dikes and sills mainly of basic composition) to this rift event. However, some of the intrusive bodies in the

south and few intrusions in the north cut the sedimentary deposits of the Upper and Middle Riphean and belong to younger igneous complexes than the products of the Mashak rifting (Kozlov et al., 2001; Knyazev et al., 2013).

OBJECTS OF STUDY

Intrusive bodies from different areas of BM were sampled (Fig. 1). Most of the studied objects in the north are located east of the Bakal-Satka fault and west of the Zyuratkul fault; in the south, they are located in the Inzer zone and Yamantau zone (Fig. 1).

The studied intrusions mainly have thicknesses from a few meters to a few tens of meters. Large intrusions were also sampled: the Main Bakal dike (91-m

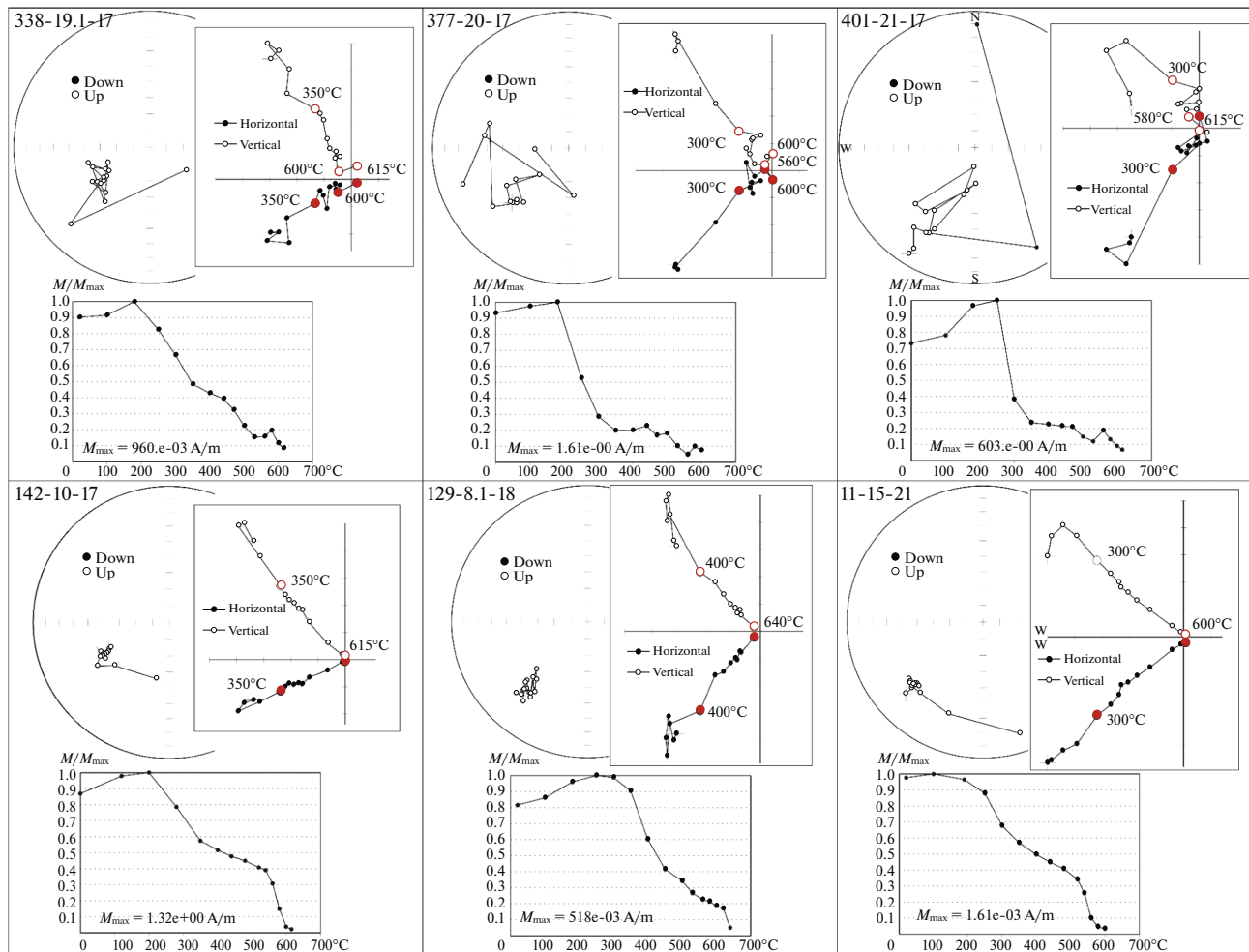


Fig. 3. Examples of thermal demagnetization results for samples from the northernmost regions near the city of Kusa (top row) and the Berdyaush village (bottom row).

thick), the Kusa-Kopan layered massif, and the Berdyaush massif. The studied intrusions are mostly composed of dolerites and gabbrodolerites, which are subject to changes in the greenschist facies of metamorphism.

In the north of BM, the studied intrusions cut the Lower Riphean Bakal and Satka formations (Figs. 1 and 2). One dike (site 25–21) cuts the Middle Riphean Kuvash Formation east of the Zyuratkul fault (Figs. 1 and 2). Two intrusive bodies cut the Avzyan (R_2) and Zilmerdak (R_3) formations west of the Bakal-Satka fault (sites 16–21 and 17–21; Figs. 1 and 2). In the south of BM, the studied intrusive bodies cut the Lower Riphean Suran Formation (stratigraphic analogue of the Satka Formation (Puchkov, 2010)) and the Upper Riphean Inzer and Minyar formations (Figs. 1 and 2). Intrusions were formed during rifting on the East European platform in the Riphean (Parnachev, 1982; Gorozhanin et al., 2008; 2014; Puchkov, 2010; Evans and Ross, 2011; Ardislamov et al., 2013; Maslov et al., 2013; Puchkov et al., 2013; Khotylev,

2018), although, for some undated bodies, a later age of emplacement cannot be completely excluded. Published isotopic ages for the sampled intrusions are the following:

- (1) Sill in Kusa town, 1360 ± 9 Ma ($^{40}\text{Ar}/^{39}\text{Ar}$, biotite; (Ernst et al., 2008));
- (2) Stock in the area of Kusa, 1318 ± 10 Ma ($^{40}\text{Ar}/^{39}\text{Ar}$, biotite; (Khotylev et al., 2019));
- (3) Dike in the area of the Berdyaush village, 1349 ± 11 Ma (U-Pb, SHRIMP II, zircon; (Khotylev et al., 2020));
- (4) “Main Bakal dike” in the town of Bakal, 1385.3 ± 1.4 Ma (U-Pb, ID TIMS, baddeleyite; (Ernst et al., 2006));
- (5) The Berdyaush massif was formed ~ 1370 million years ago, as suggested by numerous U-Pb ages (Ronkin et al., 2016). The age of the emplacement of the rapakivi-like granite phase itself is 1369 ± 13 million years;

(6) Kusa-Kopan massif, 1385 ± 25 Ma zircon age (LA-ICPMS, (Krasnobaev et al., 2006)).

Dolerites and gabbro-dolerites of the Kurgas complex (R_1/R_2), to which we attribute a significant part of the sampled objects both in the north and in the south of the Bashkirian megazone based on their relation with the host stratified rocks and isotopic dating, have ophitic, poikilitic, and gabbro-ophitic textures, while microgabbro with a fine-grained porphyritic texture is less common. The main rock-forming minerals are clinopyroxene and plagioclase, and minor minerals include biotite and hornblende, olivine, orthopyroxene, as well as quartz and potassium feldspar as a granophyre aggregate. Among the accessory minerals, the most common are apatite, magnetite, titanomagnetite, and ilmenite (Nosova et al., 2012). All rocks have secondary changes in greenschist metamorphic facies: chloritization, saussuritization, partially albitization; occasionally, aggregates of chlorite, biotite and amphibole occur. In the area of the Berdyaush village, dykes cutting the Berdyaush massif of rapakivi-like granites itself are much stronger altered than the intrusions localized in the host dolomites and marbles of the Satka formation.

The gabbroids of the Inzer complex have doleritic texture, sometimes taxitic structure due to the zones of different crystal sizes. We attribute to this complex some of the objects sampled in the south of BM, which cut the Late Riphean strata, and, possibly, a part of the northern intrusions. The main rock-forming minerals are chloritized, partially biotitized clinopyroxene and saussuritized plagioclase, and accessory minerals are titanomagnetite and apatite (Khotylev, 2018).

A more detailed analysis of the petrography and geochemistry of the intrusive bodies of the Bashkirian megazone is presented in (Nosova et al., 2012; Knyazev et al., 2013; Kovalev et al., 2013; Khotylev, 2018; 2020).

Known datings of the secondary changes, possibly associated with regional low-temperature metamorphism in the Bashkirian megazone, give three groups of ages. Some of the datings refer to the end of the Riphean–Vendian, other ages correspond to the Middle–Paleozoic, and the last group spans the end of the Paleozoic. Besides, there are datings from relatively local manifestations of hydrothermal processes that occurred, however, long before the Paleozoic folding, in the Riphean and Vendian (Maslov et al., 2001; Puchkov, 2010) and are not considered in detail here.

First cluster of datings: Krasnobaev et al. (2006) report the age of low-temperature changes in the gabbro of the Kusa–Kopan massif (one of the objects of our study) at 651 ± 30 Ma. Similar age ranges are typical of granitoids of the Ryabinovka and Gubenka massifs, which are a part of the same Middle Riphean Kusa–Kopan intrusive complex (Krasnobaev et al., 1970; Krasnobaev, 1986).

Second cluster: in the area of the Inzer river (southern intrusions, regions 5 and 6), there is an Ar–Ar age for a dyke of relatively fresh dolerites of 403 ± 17 Ma (Ernst et al., 2008). Puchkov et al. (2011) present a Paleozoic age (U–Pb, zircons) in the range of 435–455 Ma for both southern and northern intrusions of the Bashkirian megazone. For these ages, there are two possible interpretations: the age of intrusions emplacement or the age of greenschist metamorphism (Puchkov et al., 2011).

Third cluster: for the sill exposed in the Suran quarry and also studied in this work (located in region 6), there is an age of 298 ± 6 Ma ($^{39}\text{Ar}/^{40}\text{Ar}$; Kurtukova et al., 2022) estimated from the closure of the feldspar isotopic system from gabbroids, which probably corresponds to the age of secondary changes. For the Yamantau gabbrodolerite-picrite dikes complex, located in the southern part of the sampling area, there are zircon ages of 284 ± 2 and 292 ± 2 Ma (U–Pb, (Knyazev et al., 2013)). Primary dating data are not provided in the cited paper. Since other igneous bodies of this age are not known for this territory, the formation of mafic and ultramafic dike complexes is not typical for collisional settings. At the same time, Riphean intrusions formed during rift magmatism are widespread throughout the Bashkirian megazone, and we associate these Late Paleozoic ages with the time of the secondary alteration.

Thus, the early stages of metamorphism could have occurred as early as the Late Riphean–Vendian, (which is also described in (Glasmacher et al., 2004; Puchkov, 2010)). Besides, there are two more Paleozoic clusters: 403–455 and 284–298 Ma.

SAMPLING AND LABORATORY PROCEDURES

Oriented samples for paleomagnetic studies were collected in two ways: (i) manually and (ii) using a special portable drilling device. The orientation of the samples was carried out using a magnetic compass with constant monitoring of the possible influence of highly magnetic rocks on the compass needle. The local magnetic declination was calculated from the IGRF model (International Geomagnetic Reference Field, 13th Generation; http://www.geomag.bgs.ac.uk/data_service/models_compass/igrf_calc.html). From eight to 20 samples were taken from each site. The total number of oriented samples collected during four field seasons was ~1000 samples.

Laboratory paleomagnetic studies and processing of demagnetization results were carried out in the laboratory of Main Geomagnetic Field and Rock Magnetism at the Schmidt Institute of Physics of the Earth of the Russian Academy of Sciences (IPE RAS). All samples were subjected to stepwise thermal demagnetization until complete remanence removal (8–17 steps), which was achieved in most cases at tem-

peratures of 540–680°C, or until a chaotic paleomagnetic record appeared, associated with the formation of new magnetic phases during thermal demagnetization. Samples were demagnetized in non-magnetic furnaces MMTD-80 and MMTD24 with a residual magnetic field inside the oven of at most 5–10 nT. In a number of cases, for testing, sister samples were demagnetized by alternating magnetic field. The remanent magnetization of the samples was measured on a JR-6 AGICO spinner magnetometer or on a 2G Enterprises cryogenic magnetometer. Remanent magnetization measurements were processed using Enkin' program (Enkin, 1994) and Remasoft software (Chadima and Hrouda, 2006) implementing principal component analysis method to isolate the magnetization components according to (Kirschvink, 1980). The resulting paleomagnetic data were analyzed using Fisher statistics (Fisher, 1953). Measurements of the temperature dependence of magnetic susceptibility were carried out on a AGICO kappabridge MFK-1FA with a CS3 thermal control unit, in air at a heating/cooling rate of 11–13°C/min. Measurements were conducted on powder of crushed samples. The temperature dependences of saturation magnetization and remanent saturation magnetization $J_s(T)$ and $J_{rs}(T)$ were measured on 1-cm³ cubic samples on a vibrating-sample thermomagnetometer designed by Yu.K. Vinogradov. The J_s was measured in the magnetic fields in the range of 450–520 mT at a heating/cooling rate of 1°C/s. J_{rs} was acquired in a field of 1 T, and the heating/cooling rate was 1°C/s.

PALEOMAGNETIC RESULTS

In the component analysis of magnetization, we isolated a high- or medium-temperature component identified in 46 out of 83 sites (in the case of thin bodies, as a rule, one site = one intrusive body; in the case of thick bodies such as the Main Bakal dike, several sites are sampled in different parts of one intrusion). This component has southwestern declinations, moderate inclinations, and reversed polarity, and is the only stable remanence component in most of the studied intrusions. In addition, a low-temperature component is isolated, but will not be considered in detail. The directions of this component are in many cases close to the present magnetic field; this component is destroyed at approximately 250–300°C and is probably a consequence of viscous magnetization in the modern magnetic field. Preliminary results for the Riphean intrusive bodies in the northern part of the Bashkirian megazone were published in (Latyshev et al., 2019).

To compare different regions of the BM and estimate the relative tectonic movements of individual blocks within the Bashkirian megazone, the bodies with the identified stable component were combined into six groups in accordance with their geographical location and the position relative to the large faults

(according to the Geological map (Kozlov et al., 2001), Fig. 1).

When estimating the quality of the magnetic record, we consider the record good if a remanence component can be unambiguously identified from the linear interval in the Zijderveld diagram (the maximal angular deviation, MAD, is $\sim 10^\circ$ or less) and from the corresponding dense group of points on the stereogram; if there are no newly formed magnetic phases during stepwise thermal demagnetization, and if the isolated component is the only stable one in the samples. We consider a record bad when the signal is chaotic, the MAD values significantly exceed 20° , the record is poorly interpretable, and mineral alterations take place during thermal demagnetization. We consider intermediate cases a paleomagnetic signal of medium quality.

In the northernmost areas (in the vicinity of the town of Kusa and the Berdyash village, regions 1 and 2 in Fig. 1), the quality of the paleomagnetic record varies mainly from medium to good and very good (Fig. 3; in samples taken from intrusions near Kusa, record quality is worse than in samples from the intrusions near the Berdyash village). In the area of Kusa, a remanence component that is demagnetized at 300–615°C is isolated. The most stable paleomagnetic record is observed in the range up to 560–580°C. In the intrusions from the vicinity of the Berdyash village, this component is isolated starting from 300°C (and higher) and is completely demagnetized at 600–640°C. In one dike (site 16-6), a mid-Riphean high-temperature component with WSW declinations and low inclinations, which is described in detail in (Latyshev et al., 2019), occurs together with the mid-temperature component with SW declinations, which is discussed in this paper.

The mean paleomagnetic direction in the area of Kusa (region 1, Table 1) was calculated for three intrusions (three sites), α_{95} in the geographical coordinate system (modern, in our case post-folding) is 10.1° , in the stratigraphic system (ancient, with the correction for bedding of the host rock) it is 16.4° . The mean for the Berdyash village area (region 2, Table 1) was calculated over 11 intrusions (10 sites, intrusions 13–17 and 14–17 are combined into one site, the medium-temperature component of dike 16-6 was not included in the calculation because the spectrum of blocking temperatures in this component is probably partially overlapped by the high-temperature primary component), α_{95} is 7.5° in the geographical system and 15.4° in the stratigraphic system.

In the central part of the Bashkirian megazone, in the vicinity of the town of Bakal (region 3 in Fig. 1) and the Sibirka settlement (region 4 in Fig. 1), the paleomagnetic record is often of poor quality while a good paleomagnetic signal is also found (Fig. 4). In sites near the town of Bakal, a medium-high temperature component with SW declinations is identified in

Table 1. Site-mean directions of the Late Paleozoic component of the regions and region-mean directions

No.	Site no.	Site coordinates	N	D_G	I_G	D_S	I_S	K	α_{95}
Region 1 (Kusa)									
1	19.1-17	N 55°19'19.07" E 59°26'36.97"	13	229.8	-44.8	224.3	-64.6	12.5	12.2
2	20-17	N 55°24'24.16" E 59°27'32.10"	5	223.6	-34.5	272.4	-71.2	17.4	18.8
3	21-17	N 55°21'27.10" E 59°30'13.60"	4	227.7	-45.6	222.2	-66.3	40.5	14.6
Mean direction over region 1 (Kusa)									
		"Kusa"	3	226.9	-41.7			149.1	10.1
		"Kusa"	3			236.4	-68.9	57.7	16.4
Region 2 (Berdyash settlement)									
1	10-17	N 55°09'23.51" E 59°07'41.44"	14	246.6	-32.1	239.2	11.6	36.5	6.7
2	13 + 14-17	N 55°09'14.2" E 59°08'9.9" N 55°09'2.6" E 59°08'13"	11	258.1	-30.9	244.2	-4.3	51.5	6.4
3	8-18	N 55.09591° E 59.02236°	14	227.3	-20.4	227.3	-20.4	29.4	7.5
4	9.1-18	N 55.14517° E 59.15720°	17	238.8	-42	238.8	-42	18.3	8.6
5	9.2-18	N 55.14517° E 59.15720°	4	236.5	-40.1	236.5	-40.1	205.5	6.4
6	10-18	N 55.14596° E 59.15742°	5	211.6	-26.5	211.6	-26.5	171.7	5.9
7	11-18	N 55.14629° E 59.15915°	7	239.6	-38.1	239.6	-38.1	25.1	12.3
8	16-6MT*	N 55.12830° E 59.12668°	7	229.2	-38.6	324.8	-51.8	57.4	8
9	16-6HT*	N 55.12830° E 59.12668°	9	254.9	-23.9	293.2	-30	27.6	10
10	15-21	N 55°09.141' E 59°08.342'	12	239.3	-33.7	239.3	-33.7	53.5	6.0
11	22-21	N 55°04.725' E 59°13.890'	10	228.0	-37.4	221.5	-33.3	108.0	4.7
12	23-21	N 55°06.664' E 59°20.044'	7	239.7	-40.5	174.3	-48.3	43.7	9.2
Mean direction over region 2 (Berdyash settlement)									
		"Berdyash"	10	236.3	-34.8			42.0	7.5
		"Berdyash"	10			229.1	-29.0	10.8	15.4
Region 3 (Bakal)									
1	1-17	N 54°56'58.8" E 58°47'58.8"	15	212.4	-18.2	216.3	-30.6	71.1	4.6
2	2-17	N 54°57'22.9" E 58°52'53.9"	8	218.9	-30.5	223.3	15.8	10.0	18.4
3	4-17	N 54°55'05.6" E 58°50'55.3"	14	246.0	-4.7	235.7	-32.1	14.6	10.8
4	5-17	N 54°55'45.53" E 58°54'14.67"	11	217.9	-34.4	199.6	4.9	28.8	8.7
5	1-18	N 54.9035° E 58.7429°	6	219.2	-46.0	219.2	-46.0	48.8	9.7
6	2.1_2.2-18	N 54°54.423' E 58°45.713'	8	219.7	-7.5	219.7	-7.5	41.8	8.7
7	2.3-18	N 54°54.423' E 58°45.713'	7	220.0	-10.1	220.0	-10.1	22.4	13.0
8	2.4-18	N 54°54.423' E 58°45.713'	11	227.4	-31.1	227.4	-31.1	33.9	8.0
9	2.5-18	N 54°54.423' E 58°45.713'	10	233.2	-22.4	233.2	-22.4	65.1	6.0
10	3-18	N 54°54.6' E 58°46.06'	15	244.8	-20.6	244.8	-20.6	21.8	8.4
Mean direction over region 3 (Bakal)									
		"Bakal"	10	225.5	-26.8			31.7	8.7
		"Bakal"	10			219.7	-19.9	8.5	17.6
Region 4 (Sibirka village)									
1	6-17	N 54°51'20.6" E 58°57'38.3"	13	247.4	-43.8	247.4	-43.8	28.0	8.0
2	7-17	N 54°55'32.1" E 58°59'41.2"	3	225.5	-46.2	255.0	-29.8	86.6	13.3
3	8-17	N 54°55'44.3" E 58°59'22.8"	13	219.8	-46.2	150.1	-81.5	28.8	7.9
4	9-17	N 54°55'41.7" E 58°58'36.1"	9	231.2	-40.6	259.3	-39.9	53.3	7.1
5	7-19	N 54.8815° E 59.03313°	14	239.1	-52.1	239.1	-52.1	4.0	22.7
6	20-21	N 54°57.743' E 58°58.219'	11	244.9	-31.5	202.9	-56.7	60.2	5.9

Table 1. (Contd.)

No.	Site no.	Site coordinates	N	D_G	I_G	D_S	I_S	K	α_{95}
Mean direction over region 4 (Sibirka village)									
		“Sibirka”	6	235.0	−43.9			59.0	8.8
		“Sibirka”	6			241.4	−53.1	11.2	20.9
Region 5 (Inzer zone)									
1	6-20	N 54°01′ 02.6″ E 57°32′ 12.5″	12	228.1	−46.7	228.1	−46.7	54.7	5.9
2	10-20	N 54°08′ 05.6″ E 57°30′ 52.9″	14	218.0	−24.9	175.2	−30.3	15.9	10.3
3	9-20	N 54°07′ 38.5″ E 57°30′ 33.4″	16	218.1	−32.9	184.4	−35.8	23.2	7.8
4	5-20	N 53°59′ 38.4″ E 57°35′ 47.6″	10	215.7	−31.4	200.0	−31.8	21.1	10.8
Mean direction over region 5 (Inzer zone)									
		“Inzer zone”	4	219.5	−34.0			64.3	11.5
		“Inzer zone”	4			195.1	−37.7	17.8	22.4
Region 6 (Yamantau zone)									
1	4-19	N 53°57′ 11.16″ E 57°42′ 45.36″	23	234.9	−39.2	251.0	−26.1	11.5	9.3
2	5-19	N 53°54′ 14.13″ E 57°38′ 15.16″	12	233.2	−39.8	141.7	−32.5	9.1	15.2
3	12-20	N 54°09′ 57.3″ E 57°46′ 03.5″	12	220.0	−33.3	352.5	−51.7	46.6	6.4
4	2-20	N 53°57′ 14.2″ E 57°43′ 49.9″	13	230.2	−36.2	247.3	−22.9	17.2	10.3
5	3-20	N 53°56′ 46.5″ E 57°41′ 55.0″	6	223.1	−34.1	186.4	−16.9	120.2	6.1
Mean direction over region 6 (Yamantau zone)									
		“Yamantau zone”	5	228.1	−36.7			184.4	5.7
		“Yamantau zone”	5			219.6	−48.8	2.3	66.6
Sites not included in the regions									
Dyke south of Zlatoust									
25-21		N 55°04.013′ E 59°37.483′	11	204.2	−51.2	209.8	0.8	12.4	13.5
Kusa-Kopan massif									
4-18		N 55.01601° E 59.25692°	17	227.3	−16.3	227.3	−16.3	50.3	5.1
Intrusive body south of Ust-Katav									
17-21		N 54°49.996′ E 58°11.180′	7	227.0	−24.7	227.0	−24.7	35.5	10.3
Intrusive body on the southern outskirts of Katav-Ivanovsk									
16-21		N 54°43.659′ E 58°12.575′	11	178.6	−53.0	230.9	−48.2	20.4	10.4
Intrusive body southwest of the Kraka massif									
6-19		N 53.27653° E 57.52342°	18	202.9	−30.5	202.9	−30.5	9.6	11.8

N is the number of samples/sites for which the direction is calculated, D_G is the declination in geographical coordinate system, I_G is the inclination in the geographic coordinate system, D_S is the declination in the stratigraphic system coordinates, I_S is the inclination in the stratigraphic coordinate system, K is the concentration, and α_{95} is the confidence interval. Site 16-6 is the dike, where both secondary and primary components were identified; MT is medium-temperature secondary Late Paleozoic component, and HT is the high-temperature Early-Middle Riphean component.

11 sites. It is isolated mainly at 440–540 and 580–615°C (sometimes up to 680°C, including in the Main Bakal dyke). In the area of the Sibirka settlement, the component is identified at even lower temperatures, starting from 300°C. For two of the five sites sampled at the Main Bakal Dyke, paleomagnetic directions with inclinations slightly lower than those characteristic of the region are obtained. The region-mean direction calculated with sites with lower inclinations is statistically indistinguishable from that calculated with-

out these sites; therefore, they were not excluded from subsequent calculations.

The mean paleomagnetic direction for the region of Bakal town (area 3, Table 1) was calculated over six intrusions (10 sites, five of them: 2.1_2.2 (2.1 and 2.2 combined into one site), 2.3, 2.4, 2.5, 3-18 sampled from the Main Bakal dike; for sites 1-17 and 4-17, the directions in the stratigraphic system were used because tilt-corrected directions are close to those expected for this component in this area, while in the geographical system, the calculated directions are sig-

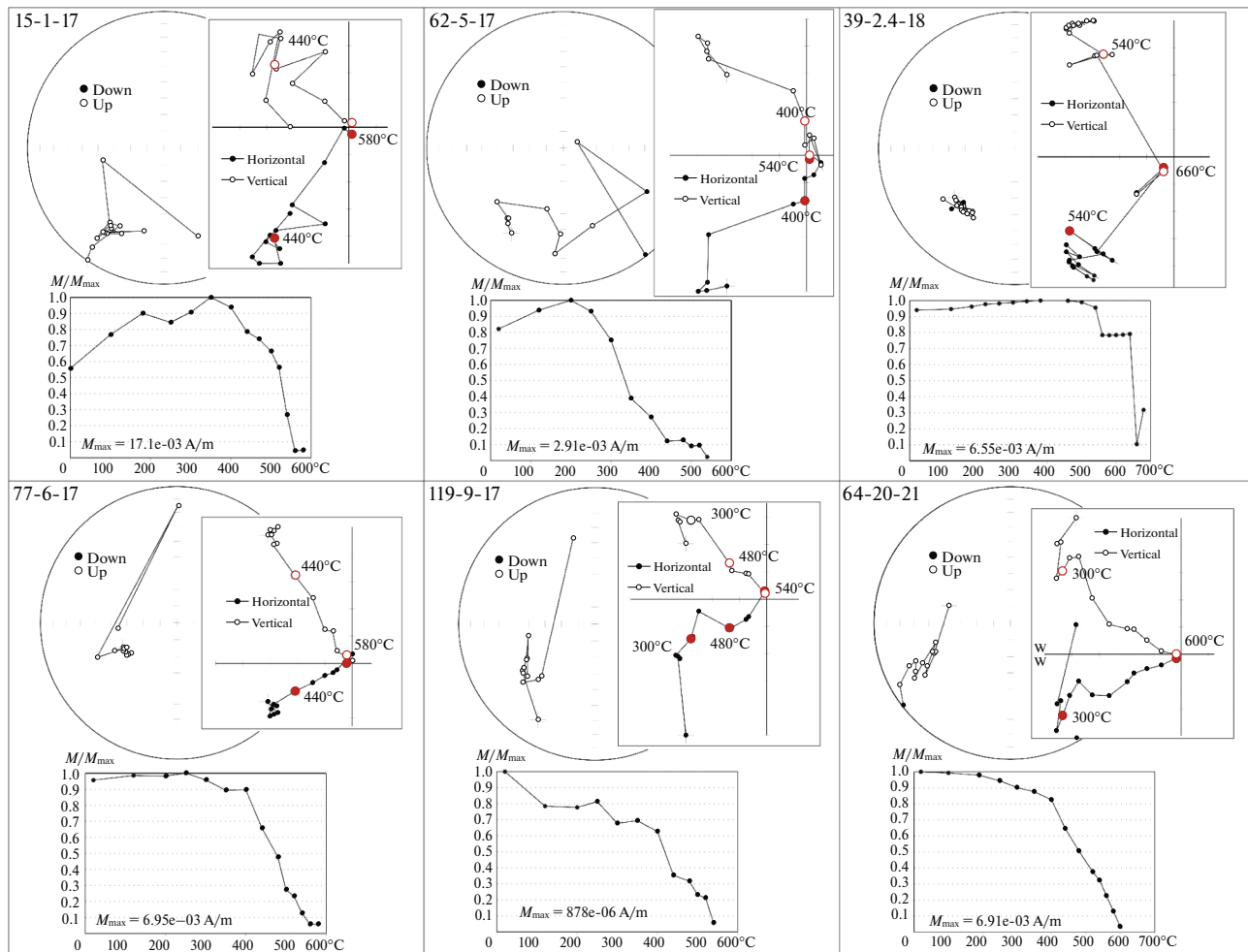


Fig. 4. Examples of thermal demagnetization results for samples from central areas near the town of Bakal (upper row) and Sibirka settlement (bottom row).

nificantly different from the expected ones). The angle α_{95} is 8.7° in the geographic system and 17.6° in the stratigraphic system. For the region of Sibirka settlement (region 4, Table 1), the region-mean direction was calculated from six intrusions (six sites); α_{95} is 8.8° in the geographical system and 20.9° in the stratigraphic system.

In the southern regions 5 (Inzer zone, 5 in Fig. 1) and 6 (Yamantau zone, 6 in Fig. 1), in some sites it was not possible to identify stable remanence components and calculate mean paleomagnetic directions due to a chaotic record that allows for no interpretation. However, in nine sites where the stable component of remanence is identified, it also has SW declinations, reversed polarity and moderate inclinations, and the quality of the paleomagnetic record is medium, sometimes good (Fig. 5).

In region 5 located in the Inzer zone (Table 1), the characteristic component is associated with the temperature range of 350–450 to 620–640°C (sometimes, up to 540–580°C), after which bias magnetization of

the samples begins, or a chaotic behavior is observed. Samples from the intrusive bodies of the Yamantau zone (region 6, Table 1) most often demagnetize to temperatures of 520–560°C (site 3–20 demagnetizes even to 480–510°C). The region-mean for region 5 is calculated over four intrusions, and α_{95} is 11.5° in the geographical system and 22.4° in the stratigraphic system. The mean for region 6 was calculated over five intrusions; α_{95} is 5.7° in the geographical system and 66.6° in the stratigraphic system.

A similar paleomagnetic component was also identified in single intrusions that were not assigned to any of the regions (Fig. 1, blue dots) due to their geographical position and the location of the relatively large faults.

In a dike exposed in a quarry near the M5 highway south of the city of Zlatoust (site 25–21), the paleomagnetic record ranges from uninterpretable to good, a component with SW declinations is isolated in the temperature range of 250–520°C/540°C (sometimes, up to 440–480°C), after which the samples are

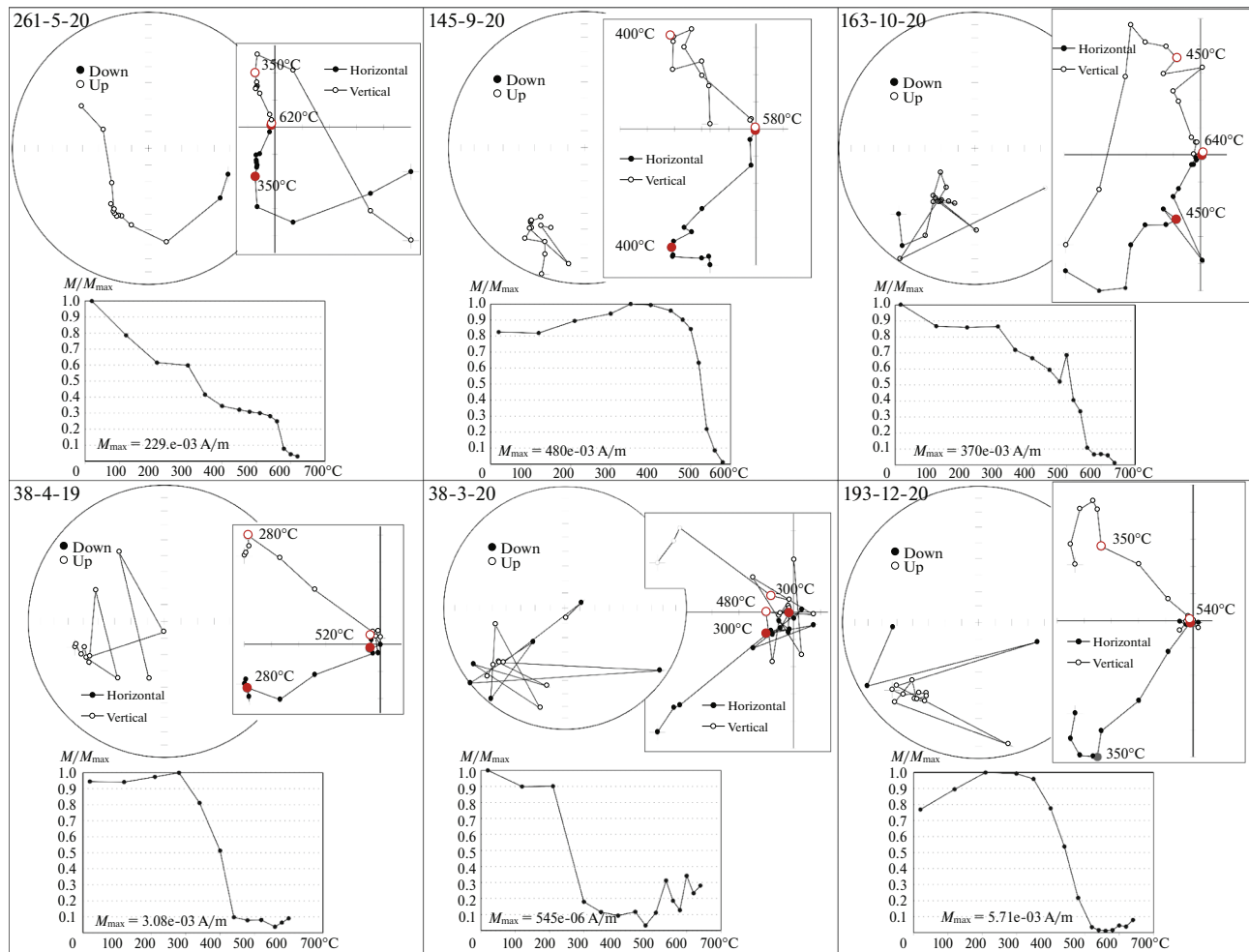


Fig. 5. Examples of thermal demagnetization results for samples from the southern regions of the Inzer zone (top row) and the Yamantau zone (bottom row).

demagnetized. The component directions have more southern declinations compared to most other sites.

In the samples collected in the Kusa–Kopan massif (in the north of the Bashkirian megazone), the paleomagnetic record is good, the stable component occurs in the temperature interval of 420–620°C/640°C and is clearly identified in one of the two sampled sites (site 4–18), where it has slightly lower inclinations compared to other directions in the area. In the second site, the directions are distributed along a great circle, probably due to the overlapping of the unblocking temperature spectra with the low-temperature viscous component.

In samples from the intrusive body south of Ust-Katav (site 17–21), the paleomagnetic record is predominantly good. The characteristic component is isolated largely in the temperature range of 300–580°C (samples are demagnetized at 540–580°C).

In the intrusive body exposed on the southern outskirts of Katav-Ivanovsk (site 16–21), the paleomag-

netic record is from poor to medium quality. The stable component mainly refers to the temperature range of 250–480°C. The directions of the component in the geographic system differ from those in other studied intrusions, but in the stratigraphic system, they are consistent with the expected values, which testifies to local folding deformations after remagnetization.

In the intrusive body southwest of the Kraka massif (site 6–19), the paleomagnetic record is of medium quality, sometimes poor. The remanence component relates mainly to the temperature range of 440–600°C. Paleomagnetic directions in samples are frequently distributed along a great circle. The direction has slightly more southern declinations compared to directions in other studied regions.

In general, the record of the magnetic signal in the studied bodies is of both poor or medium quality (more often in the south) and good. In the southern intrusions (regions of the town of Bakal, the Sibirka settlement, the Inzer zone, and the Yamantau zone), a

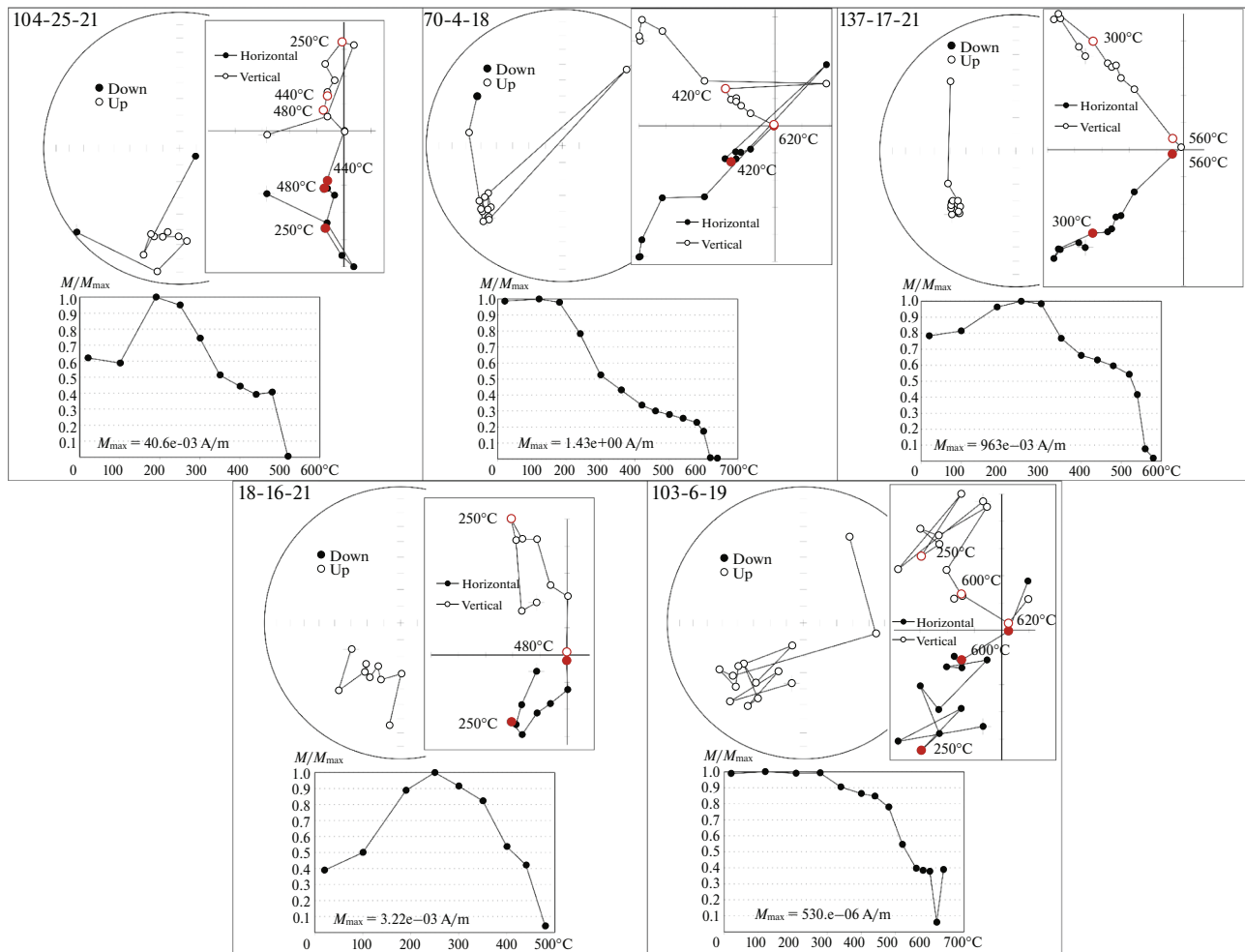


Fig. 6. Examples of thermal demagnetization results for samples from intrusions not assigned to any of the regions.

chaotic record is more common than that in the northern regions. The poor quality of the record in the areas of Bakal and the Sibirka settlement can probably be related to the position of these localities within the Bakal ore field. The best quality paleomagnetic record is most often found in the intrusions from the region of the Berdyash village. Although the nature of the record may be different, nevertheless, a component of reversed polarity, which has SW declinations and predominantly moderate inclinations, is detected in the intrusive bodies across the entire Bashkirian megazone and covers approximately the same range of the medium and high temperatures, starting from 350–400°C (less often, from 250°C—in the south). In this case, the most stable component is isolated up to 540–560°C, after which bias magnetization or the formation of new magnetic phases is often begins. Most site-mean directions are more densely grouped in the geographic coordinate system than in the stratigraphic coordinate system (Fig. 7). α_{95} for regional mean directions in the geographic system in four regions is less than 10° (regions 2, 3, 4, and 6); for two regions it

is slightly above 10° ($\alpha_{95} = 10.1^\circ$ and 11.5° for regions 1 and 5, respectively; Table 1). Therefore, we consider the isolated component post-folding, and carry out the subsequent calculations in a geographic coordinate system.

The paleomagnetic directions calculated in our study generally fall within the area of directions of the Late Paleozoic component in the Southern Urals, which have been identified in many previous works (Komissarova, 1970; Danukalov et al., 1982; Shipunov, 1993; Svyazhina et al., 2003; Iosifidi et al., 2012; Golovanova et al., 2017; 2022) (Fig. 14).

ROCK MAGNETIC PROPERTIES

According to the temperature curves of magnetic susceptibility ($K(T)$) and saturation magnetization ($J_s(T)$), the studied intrusions can be divided into two fairly different groups (Figs. 12 and 13), which are also related to the geographical location of the intrusions, northern and central-southern groups. This division of intrusions by rock magnetic properties corresponds

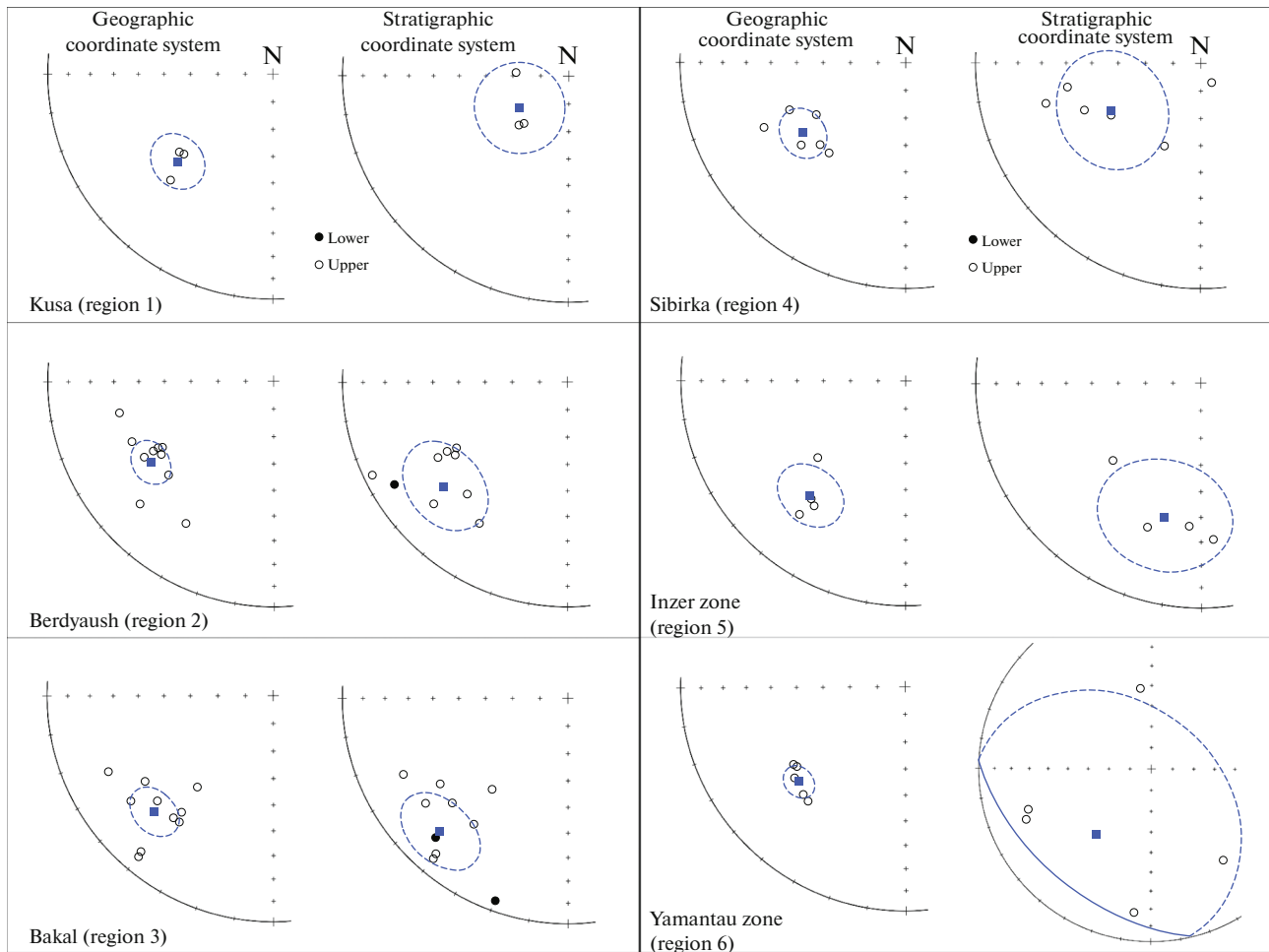


Fig. 7. Site-mean directions in the stratigraphic (pre-folding in this case) coordinate system and geographic (post-folding in this case) coordinate system for each area. Squares and dashed circles show mean directions and confidence intervals for them.

to the different quality of paleomagnetic records in the northern and southern regions.

Northern Intrusions (Regions of the Town of Kusa and Berdyaush village)

In the northern intrusions with a Late Paleozoic component (the town of Kusa, region 1, and the Berdyaush village, region 2), magnetite is clearly identified in the $K(T)$ heating curves by a sharp decrease in magnetic susceptibility near 580°C (Curie point of magnetite), sometimes with prominent Hopkinson peaks, i.e., with a sharp increase in magnetic susceptibility before the Curie point (Fig. 8). The latter can probably be associated with variations in the domain composition; a well-developed high narrow Hopkinson peak is correlated with the predominance of single-domain grains (a slightly wider Hopkinson peak) or small multi-domain grains (a narrower Hopkinson peak) (Dunlop, 1974). In sample 134-8.1-18 (region of the Berdyaush village, Fig. 8), there is no such pronounced Hopkinson peak, and magnetite here is

probably represented by larger multi-domain grains (Dunlop, 1974).

Also, oxidized or partially oxidized titanomagnetite is sometimes identified in the $K(T)$ heating curves by a rise near 200°C and a decline about $300\text{--}400^{\circ}\text{C}$ (Fig. 8). The increase in magnetic susceptibility in the region of 200°C can be also explained by a decrease in stresses associated with the initial presence of thin films of oxidation on the surface of magnetite—maghemitization (Bolshakov, 1987; Nagata, 1965). A decrease in the region of $300\text{--}400^{\circ}\text{C}$ indicates the Curie point of titanomagnetite (Nagata, 1965). After passing the Curie point of magnetite, the cooling curves do not repeat the appearance of the heating curves. In the case of this shape, the type of the heating—cooling curves is called irreversible and indicates the instability of the mineral to heating (Nagata, 1965). This fact may suggest that titanomagnetite in the studied samples is partially oxidized to form titanomaghemite and/or that it changes during heating (which means changes during thermal demagnetization).

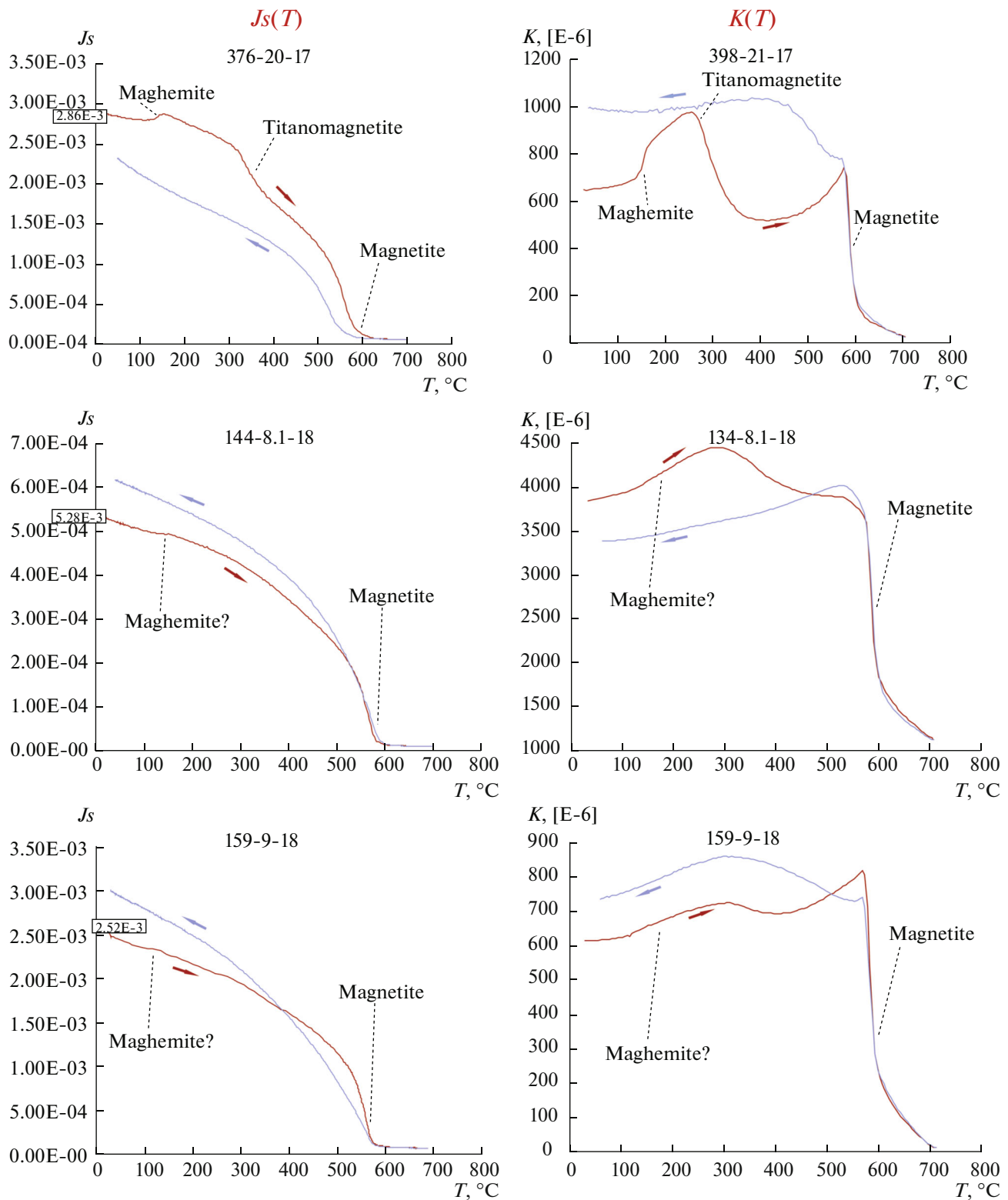


Fig. 8. Examples of temperature curves of magnetic susceptibility— $K(T)$; and temperature curves of saturation magnetization— $J_s(T)$ for northern intrusions. Heating curves are shown in red (with an arrow to the right), cooling curves are shown in blue (with an arrow to the left). The number has three digits, the first indicates the sample number, the second indicates the site number, and the third indicates the year of sampling. If the last two digits coincide, then the measurements were made for the same intrusion.

Besides, the $K(T)$ curves have a “tail” after 600°C (Fig. 8). This “tail” may be part of the paramagnetic component, or indicate the presence of hematite, which could either be initially present in the rock or formed during heating due to the oxidation of maghemite or magnetite.

To check the data obtained from the $K(T)$ curves, we compare them with the $J_s(T)$ curves for samples from the same bodies.

The $J_s(T)$ curves also show magnetite, which in most cases is stable to heating, and in some cases, there is titanomagnetite, which is identified by the decrease in the region of 300–400°C. A weak peak around 200°C may be also associated with a decrease in stress and correspond to surface maghemitization (Fig. 8; (Bolshakov, 1987; Nagata, 1965)).

Central and Southern Intrusions (Regions of the Bakal Town, Sibirka Settlement, Inzer Zone, and Yamantau Zone)

Starting from the intrusions of the Bakal region and further south, the type of rock-magnetic curves $K(T)$ and $J_s(T)$ changes: this is the second group according to rock magnetic properties (shape of the $K(T)$ and $J_s(T)$ curves). In the $K(T)$ heating curves, the magnetic susceptibility remains almost unchanged until the Curie point of magnetite, where the susceptibility drops. The cooling curves show a strong increase in magnetic susceptibility after cooling below 580°C, which apparently means strong changes that occurred in the samples as a result of heating (Fig. 9). Hopkinson peak is practically absent, and magnetite in these samples is probably represented mainly by multi-domain grains.

In the $J_s(T)$ curves of the most southern and central intrusions, only a paramagnetic signal is visible. This may be a consequence of the fact that magnetite, which is visible in the $K(T)$ curves, was formed during heating (Fig. 9). However, since the remanence component is still isolated in these objects even at high temperatures while the magnetic susceptibility does not increase or increases slightly with heating, it is likely that the paramagnetic signal in the $J_s(T)$ curves is associated with a low concentration of magnetite and also, probably, with a large number of paramagnetic minerals (which include minerals formed during greenschist metamorphism, such as, e.g., chlorite) that “clutters” the signal from the ferrimagnetic fraction.

Results of Measurement of the $J_r(T)$ Dependences

The temperature curves of the remanent saturation magnetization $J_r(T)$ (Fig. 10) do not show any particular differences between regions. The signal reaches zero in the vicinity of the Curie point of magnetite. Two declines in the region of 200 and 400°C correspond in general to one phase: oxidized or partially oxidized titanomagnetite (decrease at the Curie point

of titanomagnetite and decline at the Curie point of the more oxidized phase of titanomagnetite; oxidation of titanomagnetite can lead to an increase in its Curie point (Shcherbakov et al., 2019)). The decline of the curve in the region of 200°C can be also explained by another factor: the redistribution of vacancies in the lattice of surface maghemitized magnetite and a decrease in internal stresses (Bolshakov, 1987; Nagata, 1965).

Thus, the results of the paleomagnetic studies are generally supported by the rock magnetic studies. The studied remanence component is isolated during demagnetization at medium and high temperatures (mainly 350–400–540–580°C), which corresponds to the magnetic minerals isolated during rock magnetic studies: these are magnetite and titanomagnetite. The different nature of the rock magnetic properties of the northern and southern intrusions is comparable to the different quality of the paleomagnetic record.

In the northern regions (vicinity of the Kusa town and the Berdyash village), the magnetic fraction contains oxidized titanomagnetite and magnetite, which is mainly resistant to heating (Figs. 8 and 10). In this case, grains can be either multi-domain or pseudo-single domain.

In the Bakal region and in the south of the Bashkirian megazone, the magnetic fraction in thermale curves is predominantly composed of magnetite (Figs. 9 and 10), although there is probably also titanomagnetite (as indicated by the $J_r(T)$ graphs, Fig. 10, graph 141-10-17) since some samples are demagnetized during thermal demagnetization at temperatures below 580°C. The isolated component of remanent magnetization is most likely related with large multidomain grains.

Although, in the southern intrusions, the $J_s(T)$ curves show only a paramagnetic signal, magnetite is always distinguished in the $K(T)$ curves (Fig. 9). The worse paleomagnetic record in the southern intrusions compared to the northern ones correlates with

(a) a significant contribution of the paramagnetic signal (a paramagnetic signal in the $J_s(T)$ graphs of southern intrusions (Fig. 9), significant difference in the J_s value in the samples of northern and southern objects); (b) probably with preservation of magnetization on multi-domain grains in southern intrusions unlike northern intrusions, where during the $K(T)$ measurements, the Hopkinson peak is clearly visible, which is a sign of the presence of single-domain and/or pseudo-single-domain particles in the composition (Fig. 8, 342-19-17 and 159-9-18).

DISCUSSION

Relative Age of the Late Paleozoic Component

As was noted in the section “Paleomagnetic Results,” site-mean paleomagnetic directions in the stratigraphic coordinate system have a greater scatter than in the geographic coordinates (Fig. 11). The geo-

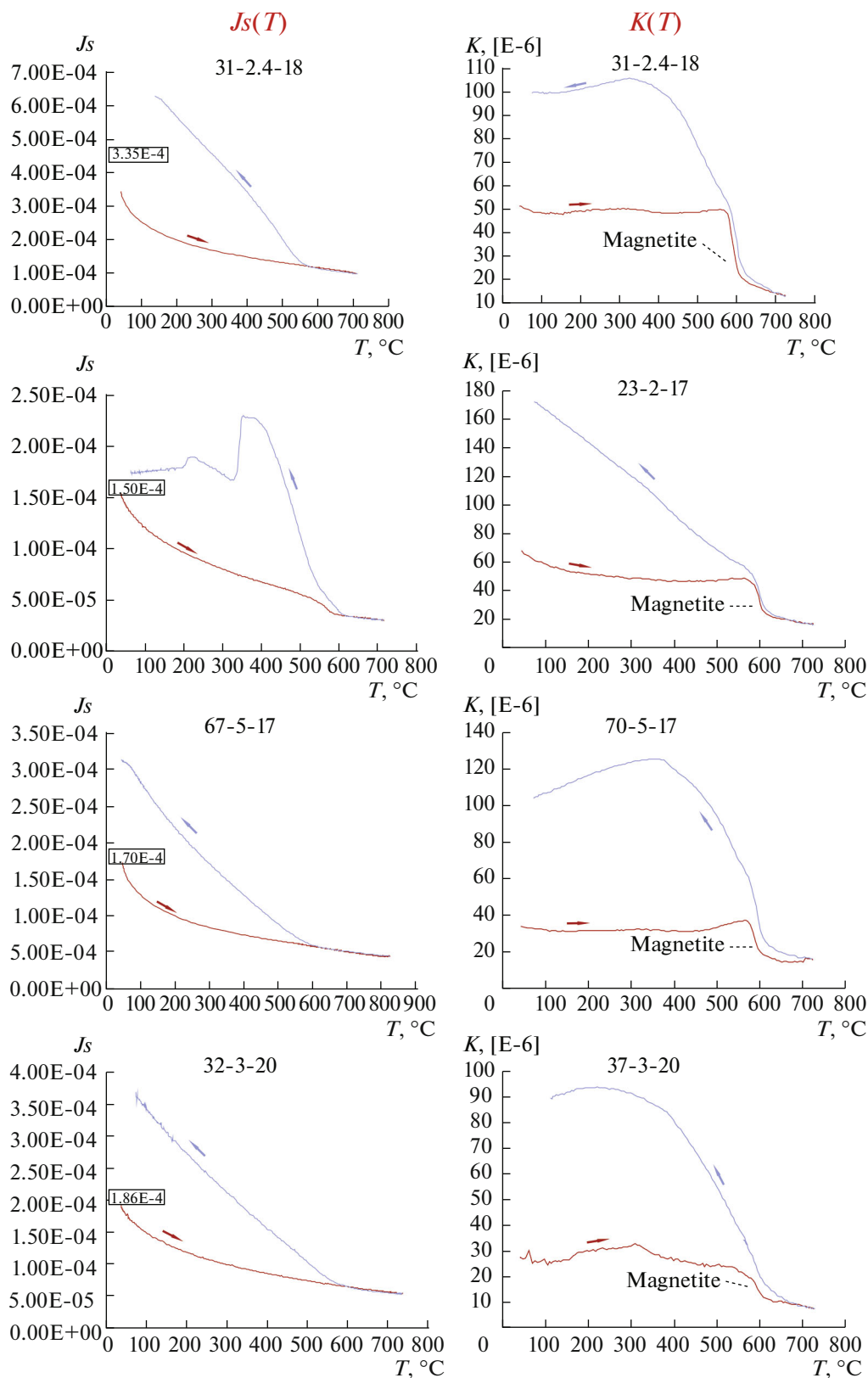


Fig. 9. Examples of temperature curves of magnetic susceptibility— $K(T)$; and temperature curves of saturation magnetization— $J_s(T)$ for the Bakal and southern areas (Inzer zone and Yamantau zone). Heating curves are shown in red (with an arrow to the right), cooling curves are shown in blue (with an arrow to the left). The number has three digits, the first indicates the sample number, the second indicates the site number, and the third indicates the year of sampling. If the last two digits coincide, then the measurements were made for the same intrusion.

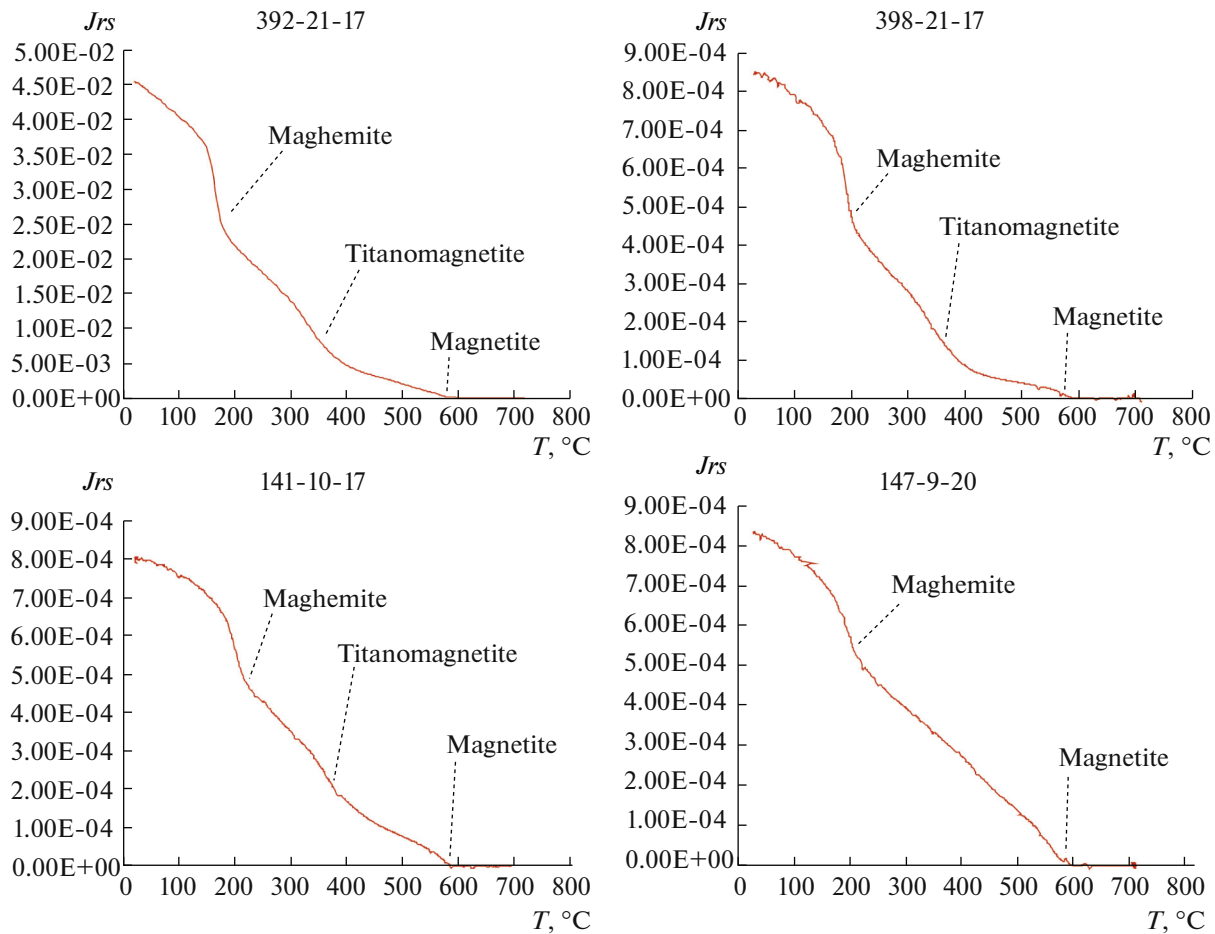


Fig. 10. Examples of temperature curves of remanent saturation magnetization— $J_{rs}(T)$ for intrusions with a Late Paleozoic paleomagnetic component (two graphs above—for intrusions of the northern group, two graphs below for objects of the southern group).

graphic coordinate system is modern, the stratigraphic system is ancient and corrected for the tilt of the host rocks. This distribution of the directions indicates that the Late Paleozoic component is post-folding, i.e., it was formed after the completion of the main folding deformations in the Southern Urals.

However, the directions calculated from sites 1-17 and 4-17 of the Bakal region (region 3, Table 1) in the geographical coordinate system differ from other Late Paleozoic directions, while in the stratigraphic coordinate system they are close to the expected Late Paleozoic directions in the geographical system. This may indicate that this region underwent deformation leading to local changes in the orientation of rocks after their remagnetization.

The Late Paleozoic paleomagnetic direction which is close to the expected one after tilt correction was also calculated for one of the westernmost sites 16-21 (southern outskirts of the town of Katav-Ivanovsk, Table 1).

The mean directions for six regions (the vicinity of the town of Kusa, the Berdyash village, the town of

Bakal, the Sibirka settlement, the Inzer zone, and the Yamantau zone) are generally close in the geographical coordinate system (Fig. 12), and sometimes they are statistically indistinguishable. For some regions, the angular difference between the directions (Table 2) is less than the critical angle. The comparison was made in the PMCALC program (Enkin, 1994), and the critical angle was calculated using the method described in (Debiche and Watson, 1995). Nevertheless, for some areas, the mean directions differ significantly. The most striking difference is observed for the directions from regions 2 and 3 (areas of the Berdyash village and the city of Bakal), which are located nearby in the central and northern part of the Bashkirian megazone. However, the directions in these regions (2 and 3) are not statistically different from the southern regions 5 and 6, which, in turn, do not differ from the northernmost region of the town of Kusa (region 1). The same distribution is typical of the poles calculated for each region (Tables 2 and 3, the pole for the region was calculated as a mean of the virtual geomagnetic poles (VGPs) for each site in the region).

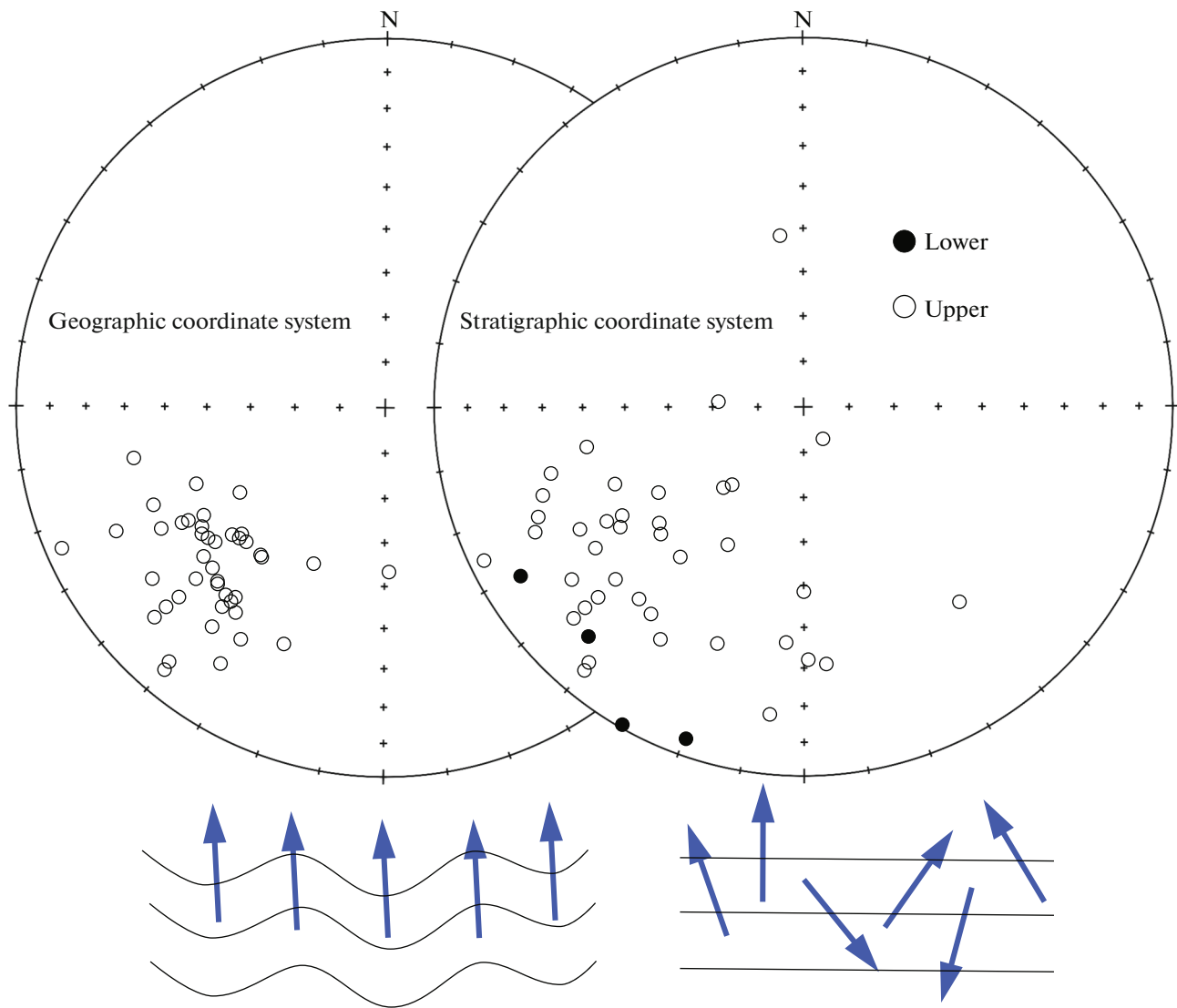


Fig. 11. Site-mean directions in the stratigraphic (pre-folding in this case) coordinate system and geographic (post-folding in this case) coordinate system.

In general, there is no obvious regularity in the distribution of directions, e.g., a gradual trend, of changes in directions from group 1 to group 6 from north to south (Fig. 12), unambiguous similarity between northern or southern regions or their differences from each other, etc. A regular distribution could indicate, for example, a rotation of blocks around a single Euler pole or a gradual migration of the remagnetization front in some direction. Since no obvious pattern can be traced, we can conclude that remagnetization occurred approximately simultaneously on the geological time scales throughout the Bashkirian megazone.

The differences in the mean paleomagnetic directions across regions can be accounted for

(1) local tectonic dislocations of blocks relative to each other;

(2) slightly different remagnetization times;

(3) insufficient averaging of secular variation of the geomagnetic field.

In general, we can consider a sufficiently close in time, predominantly post-folding remagnetization associated with the processes that affected the entire Bashkirian megazone, after which significant dislocations did not occur within it. However, the existing data indicate the possibility of local folding deformations in some areas even after remagnetization.

Absolute Age of the Late Paleozoic Component, Calculation of the Paleomagnetic Pole

The paleomagnetic pole corresponding to the Late Paleozoic component (Table 3) was calculated from the mean VGP for each region: $Plong = 171.6$, $Plat =$

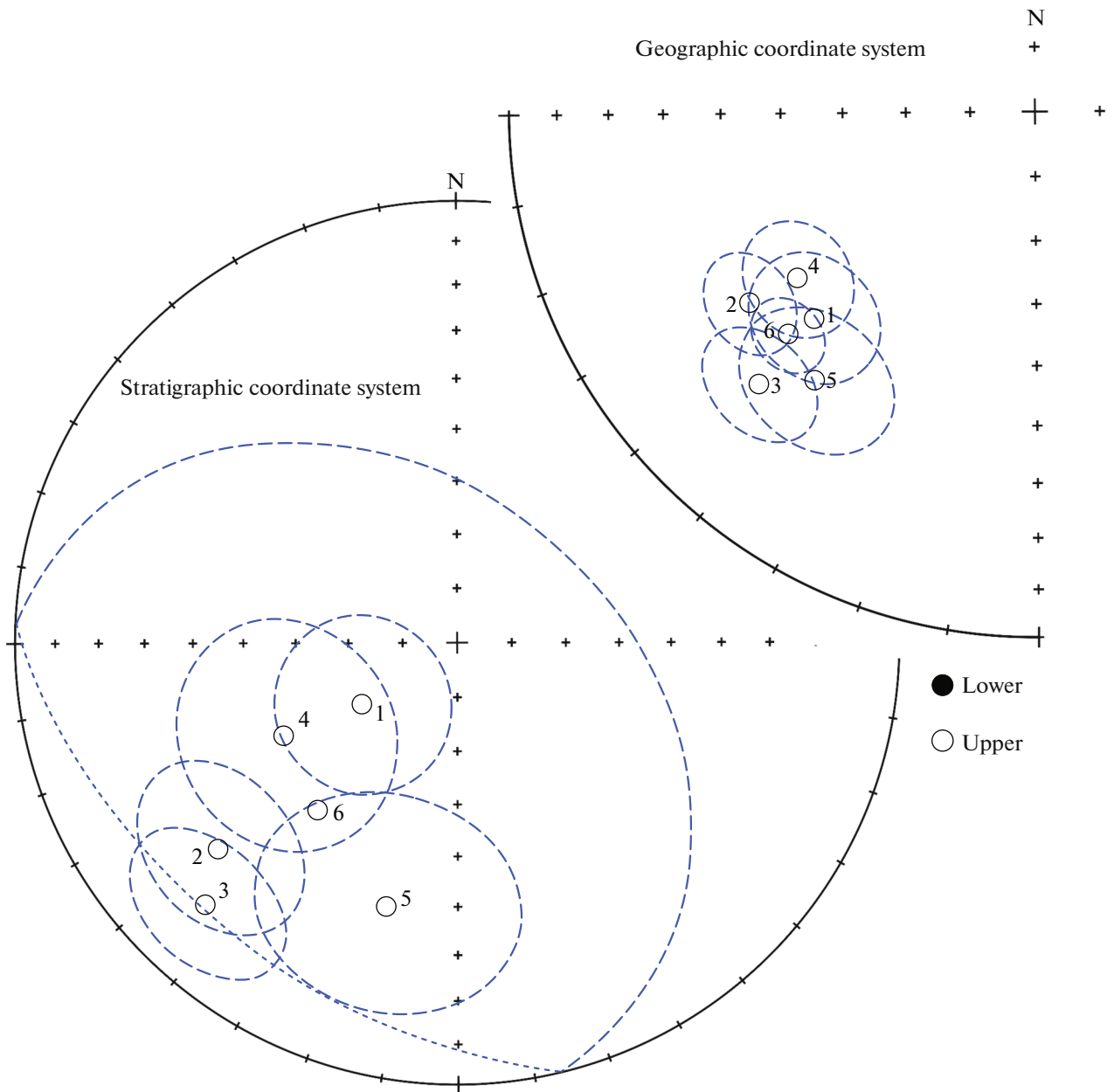


Fig. 12. Region-mean paleomagnetic directions in the stratigraphic coordinate system and geographic (post-folding) coordinate system.

39.9, $\alpha_{95} = 5.9$ (six regions, 38 sites, without sites not related to one of the areas).

To determine the age of the pole calculated from the Bashkirian megazone, we compared it with the poles used in (Torsvik et al., 2012) to calculate the apparent polar wander path (APWP) for Stable Europe. Among the poles for stable Europe, we selected those closest to the pole we obtained; the ages of the selected poles fall within the time interval predominantly of 280–312 Ma; and there are also two poles close to the calculated one, with ages of 275 and 260 Ma (Fig. 13). Among the closest ones, we selected

poles obtained from the currently available primary data (almost all, with the exception of single publications, where primary data are not provided or where access to the publications is restricted). Among the latter, we selected the poles obtained with a complete paleomagnetic demagnetization, with $\alpha_{95} < 10^\circ$ and reliable age determination. After selection, 15 poles remain, which lie in an almost continuous time interval 280–301 Ma (the difference between poles is at most 5 Ma) and one pole with an age of 260 Ma (Table 3, Fig. 14). The 260 Ma pole meets the reliability criteria, but it was excluded from the final sample because it

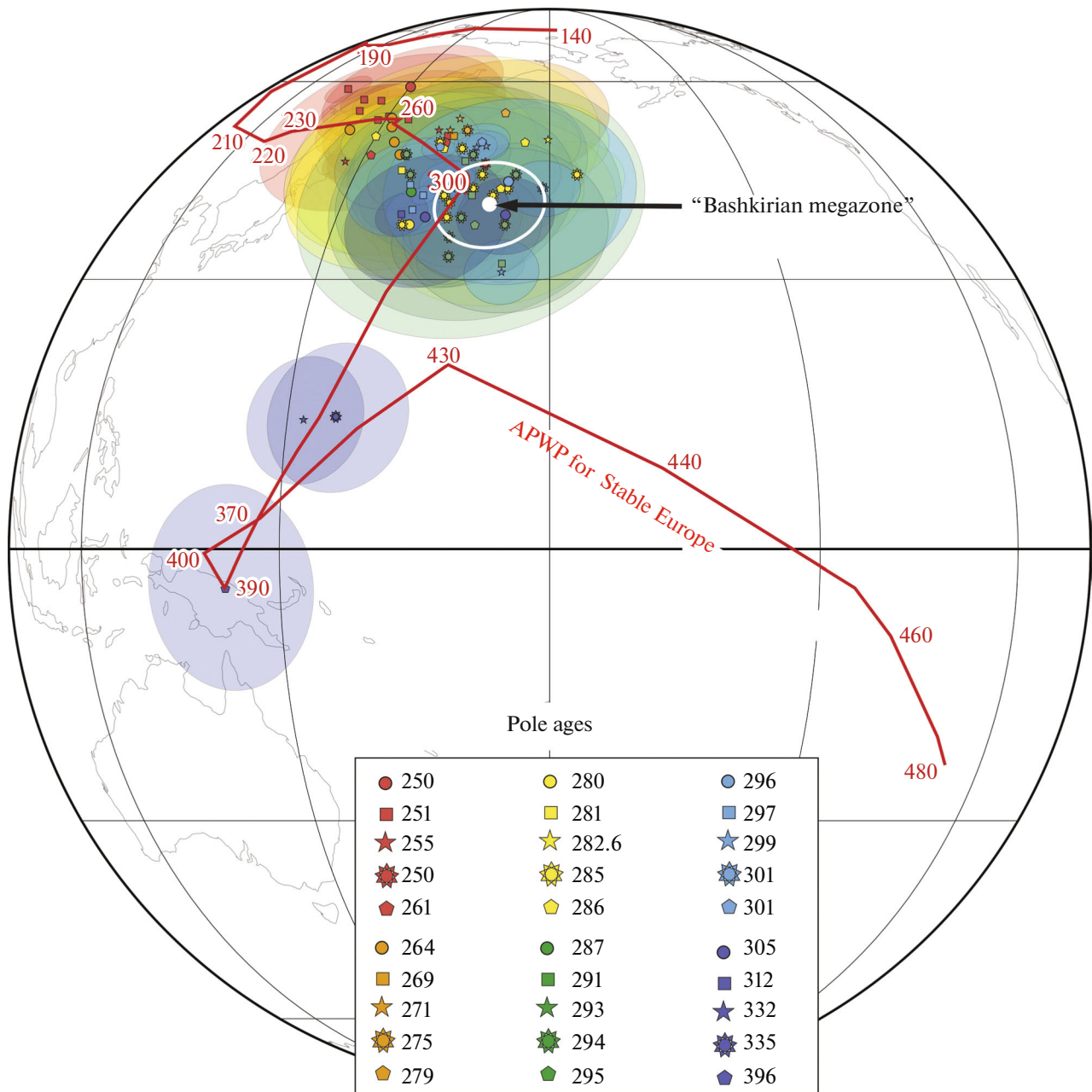


Fig. 13. Pole calculated for six regions of the Bashkirian megazone. The red line is a segment of APWP for Stable Europe with an age of 480–140 Ma (based on (Torsvik et al., 2012)). All poles of the age interval of 250–396 Ma (used in (Torsvik et al., 2012) to construct the APWP of Stable Europe) are also shown to visually display the proximity of the pole we calculated to the poles with ages of ~280–312 Ma (yellow-blue -green area).

differs significantly in age from the others selected; in addition, it differs in paleocoordinates from the coeval poles (as was indicated by Bazhenov et al. (2008), who published the pole). Most poles in the final sample corresponds to the age of 285 Ma (six poles against one or two poles with each of the other ages), but this is due to the initially large number of poles aged 285 Ma. Thus, the final comparison was made with the selected poles corresponding to age of 280–301 Ma.

The pole calculated for the Bashkirian megazone is statistically indistinguishable (angular difference is $1.9^\circ \pm 5.1^\circ$) from the average of the 15 selected poles for stable Europe with ages of 280–301 Ma (Table 3, Fig. 14), which corresponds to the end of the Late Carboniferous–Early Permian.

We also calculated the mean pole for 43 sites of the Bashkirian megazone (with sites that were not included in any of the regions): $P_{long} = 172.2$, $P_{lat} =$

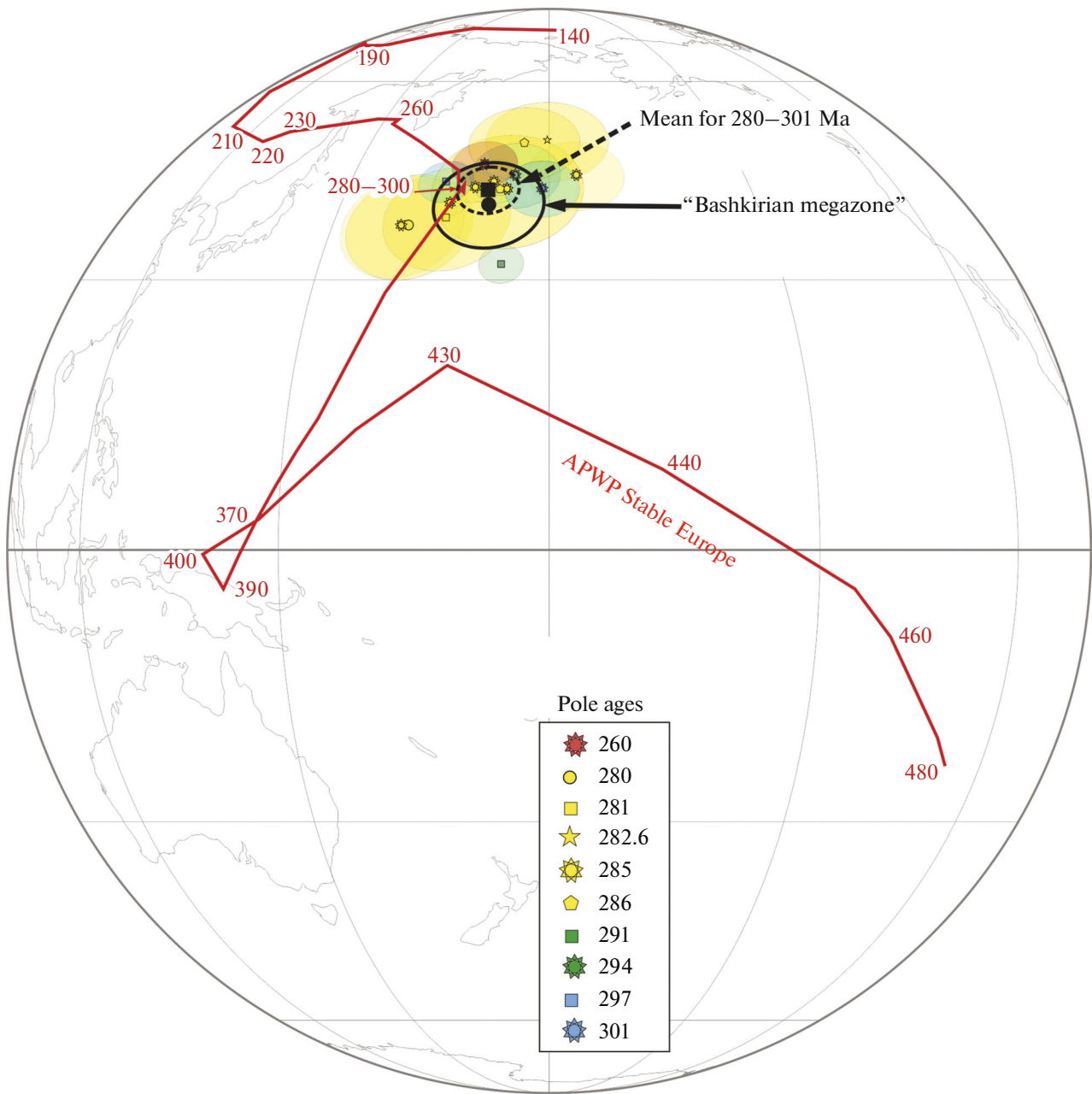


Fig. 14. Pole calculated from six regions of the Bashkirian megazone and its comparison with selected poles for Stable Europe (used in (Torsvik et al., 2012) for APWP of Stable Europe) with age of 280–301 Ma (ages are given below on the globe in the frame). The red line is the APWP of Stable Europe according to (Torsvik et al., 2012).

39.4, and $\alpha_{95} = 3.5$. This pole represents the mean of all VGPs from each point. The pole calculated with the inclusion of sites which are outside the distinguished the regions and the pole calculated as the mean for six regions are almost identical. For the comparison with the APWP of Stable Europe, the mean pole for the regions was used because, in any case, regions containing many sites will make a larger contribution to the mean compared to single sites located

at a considerable distance from other intrusions and separated from all regions by large faults.

Thus, the Late Paleozoic remanence component was formed ~280–301 million years ago, after which the Bashkirian megazone did not experience significant horizontal displacements relative to the East European platform. Besides, there were no significant dislocations of blocks within the Bashkirian megazone itself. However, there may have been local horizontal

Table 2. Angular difference between region-mean paleomagnetic directions in the geographic coordinate system

Angles between mean directions					
	1 “Kusa”	2 “Berdyash”	3 “Bakal”	4 “Sibirka”	5 “Inzer zone”
1 “Kusa”					
2 “Berdyash”	$9.3^\circ \pm 7.6^\circ$				
3 “Bakal”	$14.4^\circ \pm 8.2^\circ$	$11.5^\circ \pm 8.3^\circ$			
4 “Sibirka”	$4.9^\circ \pm 8.0^\circ$	$8.2^\circ \pm 8.1^\circ$	$18.2^\circ \pm 8.7^\circ$		
5 “Inzer zone”	$8.6^\circ \pm 8.8^\circ$	$13.1^\circ \pm 8.9^\circ$	$7.5^\circ \pm 9.4^\circ$	$14.8^\circ \pm 9.2^\circ$	
6 “Yamantau zone”	$3.9^\circ \pm 6.5^\circ$	$6.1^\circ \pm 6.6^\circ$	$9.4^\circ \pm 7.3^\circ$	$8.1^\circ \pm 7.1^\circ$	$6.4^\circ \pm 7.9^\circ$
Angles between mean poles					
	1 “Kusa”	2 “Berdyash”	3 “Bakal”	4 “Sibirka”	5 “Inzer zone”
1 “Kusa”					
2 “Berdyash”	$9.4^\circ \pm 6.7^\circ$				
3 “Bakal”	$6.3^\circ \pm 6.5^\circ$	$9.8^\circ \pm 7.6^\circ$			
4 “Sibirka”	$11.0^\circ \pm 7.6^\circ$	$7.0^\circ \pm 8.5^\circ$	$15.6^\circ \pm 8.4^\circ$		
5 “Inzer zone”	$4.4^\circ \pm 6.8^\circ$	$13.5^\circ \pm 7.8^\circ$	$5.8^\circ \pm 7.7^\circ$	$15.8^\circ \pm 8.6^\circ$	
6 “Yamantau zone”	$4.2^\circ \pm 6.4^\circ$	$4.2^\circ \pm 7.5^\circ$	$7.1^\circ \pm 7.3^\circ$	$7.0^\circ \pm 8.3^\circ$	$8.6^\circ \pm 7.6^\circ$

In the combination, for example, $10^\circ \pm 9.3^\circ$, 10° is the angular difference, and 9.3° is the critical angle. The comparison was made in the PMCALC program (Enkin, 1994), and the critical angle was calculated using the method described in (Debiche and Watson, 1995).

movements, and, at least in the Bakal region and to the west, even local folding deformations.

The identified Late Paleozoic component is secondary because the age of the formation of the studied intrusive bodies is Riphean. However, there are Ar-Ar and U-Pb ages that lie in the time interval of 284–298 Ma, which we interpret as the age of secondary low-temperature changes, probably the age of the last stage of greenschist metamorphism (more detail are in the section “Geology of the region and objects of study”). The ages in the range of 284–298 Ma are in good agreement with the established age of the acquired remanence component. At the same time, greenschist metamorphism can play a role in both thermoviscous and chemical remagnetization, but this issue may be the topic of a separate paper.

The data obtained in this study are consistent with the previous results (Levashova et al., 2013; Golovanova et al., 2017; 2022) regarding the lack of rotation of the Southern Urals blocks relative to the East European platform. Also, throughout the Southern Urals, starting from the megazone of Foreland Thrusts and ending with the Central Magnitogorsk zone, the time of acquisition of the secondary component coincides, and no obvious regularity can be traced in the nature of its distribution (Fig. 15). From this, we can conclude that in this part of the Southern Urals, the secondary component was acquired all over the region, approximately simultaneously, and its formation was associated with the processes that affected the entire studied territory at that time.

Paleozoic Collision in the Southern Urals and the Paleomagnetic Constraints of Its Processes in Time and Space

The processes of orogenesis in the Southern Urals are associated with the time interval between the Late Devonian and Late Permian, although in the Early Jurassic and Pliocene-Quaternary time, there was also a short-term recommencement of vertical motions (Brown et al., 1997; 2000a; Brown and Spadea, 1999; 2000b; Puchkov, 2009; 2010).

The beginning of the main stage of deformation in the Southern Urals is correlated with the end of the Devonian based on data on the age of high-pressure metamorphism of the eclogite-glaucophane schist Maksyutov complex, 385–365 Ma (Givetian-Famenian), and the beginning of the Zilair flysch sedimentation at the end of the Frasnian (Matte et al., 1993; Shatskii et al., 1997; Hetzel et al., 1998; Beane and Connelly, 2000; Brown et al., 2000a; 2000b; 2001; Romaine et al., 2000; Glodny et al., 2002; Puchkov, 2010). The tectonic thrust sheets of the Zilair thrust and the Uraltau zone, which includes the Maksyutov complex, in modern coordinates are located southeast of the Bashkirian megazone. In the Late Devonian in the Southern Urals, a collision stage began, associated with the accretion of the Magnitogorsk volcanic arc to the East European Platform, which ended in the Early Carboniferous (Puchkov, 2000; 2010).

During the Carboniferous, stages of compression were followed by stages of extension. The latter corresponds to the time gap between collisions of the island

Table 3. Poles for stable Europe that were used in (Torsvik et al., 2012) to construct the apparent polar wander part of the Baltic pole in the Paleozoic and the calculated pole for six regions (38 sites) of the Bashkirian megazone (in a geographic coordinate system)

Objects	<i>N</i>	Plong	Plat	α_{95}	Age, Ma
Red terrigenous rocks of the western part of the Cisuralian foredeep (Bazhenov et al., 2008)	94	170.2	45.6	3.5	260
Rhyolites of the Bohemian Massif, Germany (Thomas et al., 1997)	10	161	37	7	280
Sarna alkaline intrusions, Sweden (Smith and Piper, 1979)	19	166	38	6.9	281
Trachyte dikes, Ukraine (Yuan et al., 2011)	19	179.7	49.4	6.5	282.6
Volcanics of the Central European Basin (north), Poland (Nawrocki, 1997)	10	174	42	8.1	285
Volcanics of the Central European Basin (center), Poland (Nawrocki, 1997)	54	172	43	3.2	285
Sedimentary rocks of the Central European Basin (north), Poland (Nawrocki, 1997)	29	184	44	5.1	285
Sedimentary rocks of the Central European Basin (center), Poland (Nawrocki, 1997)	6	160	37	6.8	285
Krkonoše oil shale, Czech Republic (Krs et al., 1992)	50	166.2	40	1.8	285
Sedimentary rocks of the Lodève basin, France (Mefwbet and Guillaume, 1988)	65	169.4	42.2	2.2	285
Rhyolites of the Black Forest, Germany (Edel and Schneider, 1995)	18	173	42	1	286
Volcanic rocks of the Black Forest, Germany (recalculated in (Torsvik et al., 2012) based on data from (Konrad and Nairn, 1971))	–	176	49	5.9	286
Stabbene Sill, Norway (Sturt and Torsvik, 1987)	33	174	32	2.4	291
Volcanic rocks of Krakow, Poland (Nawrocki et al., 2008)	–	175	44	4.8	294
Red mudstones of the Donets basin, Ukraine (Iosifidi et al., 2010)	28	164	43	3	297
Sedimentary rocks of the Donetsk basin, Ukraine (Iosifidi et al., 2010)	24	179	42	4	301
Mean over 15 poles for stable Europe	–	171.3	41.8	3.3	
Our data					
“Kusa”	3	174.6	42.8	7.4	
“Berdyash”	10	166.5	35	7.5	
“Bakal”	10	179.3	36.3	7.2	
“Sibirka”	6	159.2	40.8	9.6	
“Inzer zone”	4	181.1	43.5	9.2	
“Yamantau zone”	5	169.6	39.1	7.8	
Mean over six regions of the Bashkirian megazone	6 (38)	171.6	39.9	5.9	
Mean over 43 sites of the Bashkirian megazone	43	172.2	39.4	3.5	

N is the number of sites/regions, Plong is the longitude, Plat is the latitude of the paleomagnetic pole, and α_{95} is the confidence interval.

arc–continent type (accretion Magnitogorsk arc) and the continent–continent type (East European and Kazakhstan continents). Carboniferous rift complexes are represented in the Central Magnitogorsk zone, the axial part of which is considered as the Magnitogorsk–

Bogdanov graben (Puchkov, 2000; Salikhov and Yarkova, 1992). In the Bashkirian Age of the Middle Carboniferous, a collision of the East European and Kazakhstan paleocontinents occurred. In the Moscovian Age, subduction completely ended in the South-

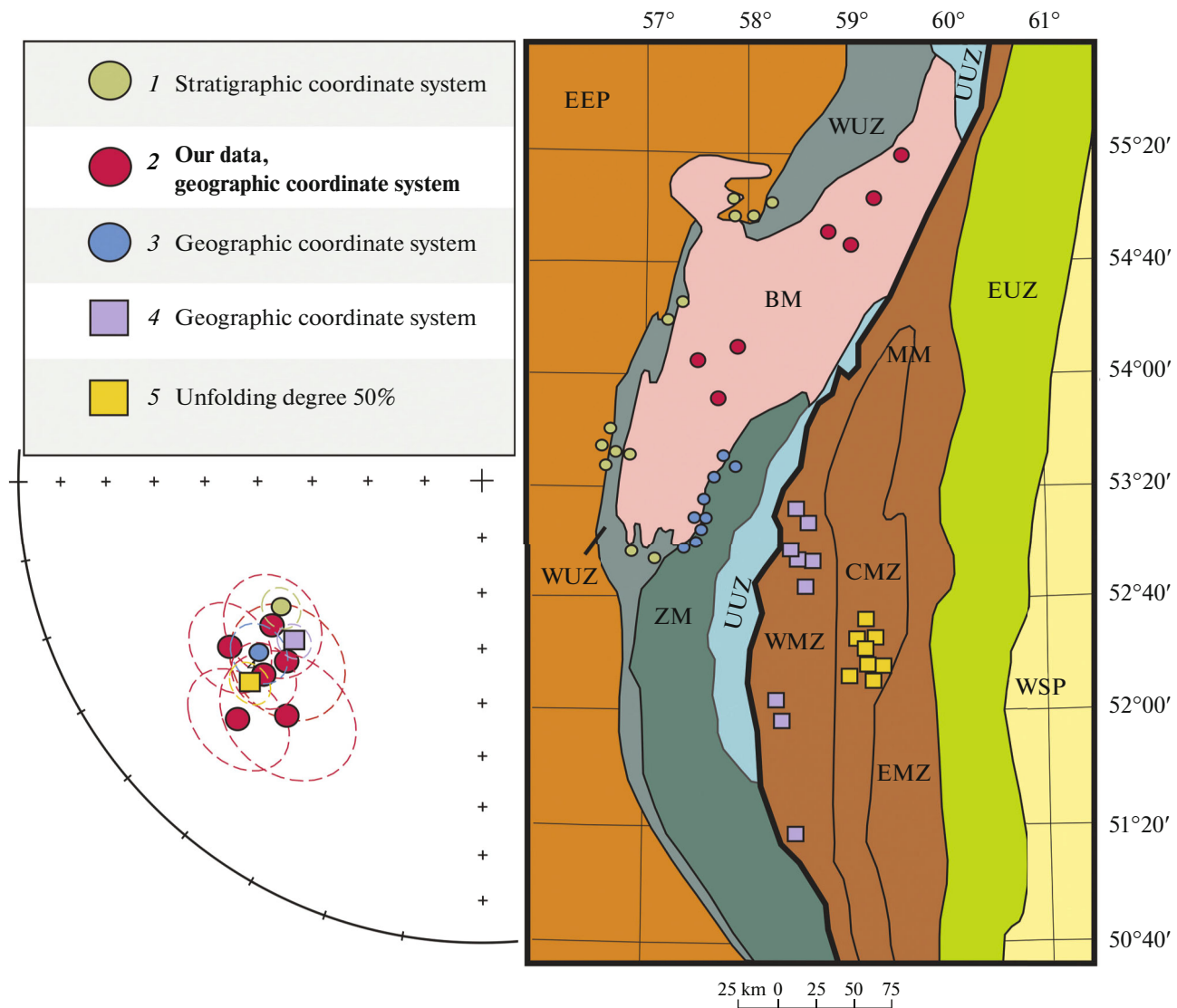


Fig. 15. Comparison of mean directions for six regions of the Bashkirian megazone with previously published data on the secondary Late Paleozoic component of the Southern Urals. On the right is a tectonic scheme of the Southern Urals (based on the works of (Golovanova et al., 2022; Kozlov et al., 2001)) with marked sampling sites (circles and squares). Tectonic units: EEP—East European Platform; WUZ—Western Uralian zone of external folding; BM—Bashkirian megazone; UUZ—Ufaley-Uraltau zone (Uraltau in the south, Ufaley in the north); MM—Magnitogorsk megazone (in it: WMZ—West Magnitogorsk zone; CMZ—Central Magnitogorsk zone; EMZ—East Magnitogorsk zone); EUM—East Uralian megazone; WSP—West Siberian plate. 1, 3–5—data from (Levashova et al., 2013; Vinogradov, 2016; Golovanova et al., 2017; 2022); 2—our data for six regions of the Bashkirian megazone.

ern Urals, the East European and Kazakhstan paleocontinents came into direct contact, and a “hard” continent–continent collision began (Puchkov, 2000; 2010; 2009).

Traces of Permian syncollisional deformations are preserved both in the cover of the Cisuralian foredeep foredeep of the East European Platform (folding is manifested in the sedimentary rocks of the cover, both Early and Late Permian, although often the dislocation of Permian and younger sediments of the Urals, and particularly in the southern regions, is associated with salt tectonics, which became active at the end of

the Permian (Puchkov, 2000; 2010)), and in the East Uralian megazone. At the Permian stage, hard collision manifested itself most intensely in the eastern part of the Urals, as suggested by large Early Permian anatectic granite plutons of the East Uralian megazone (Puchkov, 2000). Early Permian deformations of the more western part of the Urals, which includes the Bashkirian megazone and which had formed by that time the rigid passive margin of the East European Platform, are characterized as “relatively weak crowding of the Earth’s crust” (Puchkov, 2000). In Late Permian, the axis of the eroded uplift shifted to the

west compared to the early stages of the formation and development of the foredeep, and the western slope of the Southern Urals is described as the main provenance region of the material for the foredeep in the Late Permian (Puchkov, 2000). Only by the end of the Permian, collision processes attenuated (Puchkov, 2009; 2010).

In the complex history of syncollisional deformations of the Southern Urals, the age of folding in the axial part of the Bashkirian megazone compares with predominantly Late Carboniferous–Early Permian time, although Early Permian deformations in the western part of the Southern Urals are considered relatively weak compared to the processes of orogenesis in the eastern regions (Puchkov, 2000). The movement of the axis of intense deformations to the west towards the Late Permian is also described (Puchkov, 2000). However, conclusions about the Late Carboniferous–Early Permian deformations and the westward movement of the folding axis are based, among other things, on paleomagnetic data on the Late Riphean (R_3) Katav formation (Shipunov, 1991; 1995; 1998; Puchkov, 2000). Currently, the remanence of the Katav formation is considered as possibly primarily Riphean (Pavlov and Gallet, 2009). Thus, the nature of the remanence of the Katav formation is at least debatable, which deprives us of the possibility to reconstruct the Late Paleozoic history of the Southern Urals from these data.

The results of paleomagnetic studies of numerous mafic intrusive bodies of the Bashkirian megazone presented here suggest that by the beginning of the Permian, the fold-thrust structure of the Bashkirian megazone should have already formed.

Similar Late Paleozoic paleomagnetic directions are distinguished throughout the Bashkirian megazone, which has a submeridional extent of ~ 250 km. The site-mean directions and poles form a sufficiently close group in the geographic coordinate system, in contrast to the directions in the stratigraphic system. Comparison with reference poles (see (Torsvik, 2012)) for Stable Europe makes it possible to establish more accurately the time frame of the Late Paleozoic magnetic overprint of 280–301 Ma (the very end of the Carboniferous–Early Permian).

Thus, after the formation of the Late Paleozoic component 280–301 Ma, significant regional tectonic movements within the Bashkirian megazone, as well as the rotation of the Bashkirian megazone relative to the East European Platform, did not occur. Local deformations that occurred after the formation of the secondary remanence component are rarely observed within the region. In particular, in the Bakal region for two intrusions and in the west of BA near the town of Katav-Ivanovsk for one intrusion, tilt-corrected directions are close to the expected for the Late Paleozoic component, and here, local folding deformations took place even after the remagnetization.

The absence of rotation of the tectonic blocks of the Southern Urals relative to the East European Platform and the absence of significant movements after the Early Permian was described earlier. In the parts of the Southern Urals that are more eastern than the Bashkirian megazone,—in the Zilair megazone and in the West Magnitogorsk zone, a postfolding secondary Late Paleozoic component of magnetization was also identified (Levashova et al., 2013; Golovanova et al., 2017; 2022) (Fig. 15). At the same time, in the westernmost part of the Bashkirian megazone and in the Western Ural megazone of external folding, deformations occurred even after the formation of the Late Paleozoic secondary component, which in these areas is pre-folding. The synfolding, or formed shortly before the onset of deformation, Early Permian component is identified east of the West Magnitogorsk zone in the Carboniferous Bogdanov graben of the Central Magnitogorsk zone, which was a relatively young structure at the time of Permian deformations in the Southern Urals (Levashova et al., 2013; Golovanova et al., 2017; 2022) (Fig. 15). The formation time of the component in all considered areas falls within the range of ~ 270 –300 Ma. There are no regularities in the distribution of the component, i.e., the component was formed everywhere ~ 270 –300 Ma ago due to the processes manifested at that time throughout the territory, from the West Uralian zone in the west to the Central Magnitogorsk zone in the east (Fig. 15).

Thus, the available paleomagnetic data allowed us to establish that at the beginning of the Permian, regional folding deformations to the west of the Main Uralian Fault had already ended and did not resume later, except for the most western parts of the South Ural folding zone: the West Uralian zone and the bordering territories.

CONCLUSIONS

The paleomagnetic pole calculated from the Late Paleozoic component for the Bashkirian megazone coincides with the mean of 15 poles for the East European platform with the ages of 280–301 Ma. Consequently, the Bashkirian megazone did not experience displacement relative to the East European platform after ~ 280 Ma.

The Late Paleozoic secondary component of magnetization in most of the territory of the Bashkirian megazone is post-folding, i.e., after the Early Permian, the western part of the Southern Urals (at least east of the Zilmerdak fault) did not experience significant folding deformations.

Late Paleozoic remagnetization widely manifested in the Southern Urals and within the Bashkirian megazone occurred in the range of 280–301 Ma.

FUNDING

The measurements were carried out using the equipment of the Shared Research Facilities “Petrophysics, Geomechanics and Paleomagnetism” of Schmidt Institute of Physics of the Earth of the Russian Academy of Sciences under project 0144-2019-0006 supported by ongoing institutional funding.

CONFLICT OF INTEREST

The authors of this work declare that they have no conflicts of interest.

REFERENCES

- Ardislamov, F.R., Savel'ev, D.E., Snachev, A.V., and Puchkov, V.N., *Geologiya mashakskoi svity Yamantauskogo antiklinoriya (Yuzhnyi Ural)* (Geology of the Mashakskaya Formation of the Yamantausky Anticlinorium (South Urals)), Ufa: DizainPress, 2013.
- Bazhenov, M.L., Grishanov, A.N., Van der Voo, R., and Levashova, N.M., Late Permian palaeomagnetic data east and west of the Urals, *Geophys. J. Int.*, 2008, vol. 173, no. 2, pp. 395–408. <https://doi.org/10.1111/j.1365-246x.2008.03727.x>
- Bazhin, E.A. and Snachev, V.I., New data on the geological structure of the Berdyaushsky massif of granite-rapakivi (Southern Urals), *Geol. Sb.*, 2014, no. 11, pp. 15–21. <https://www.elibrary.ru/yhmfzb>.
- Beane, R.J. and Connelly, J.N., $^{40}\text{Ar}/^{39}\text{Ar}$, U–Pb, and Sm–Nd constraints on the timing of metamorphic events in the Maksyutov Complex, southern Ural Mountains, *J. Geol. Soc.*, 2000, vol. 157, no. 4, pp. 811–822. <https://doi.org/10.1144/jgs.157.4.811>
- Bogdanova, S.V., Bingen, B., Gorbatshev, R., Kheraskova, T.N., Kozlov, V.I., Puchkov, V.N., and Volozh, Yu.A., The East European Craton (Baltica) before and during the assembly of Rodinia, *Precambrian Res.*, 2008, vol. 160, nos. 1–2, pp. 23–45. <https://doi.org/10.1016/j.precamres.2007.04.024>
- Bolshakov, V.A., Gapeyev, A.K., and Yasonov, P.G., Piezochemical remanent magnetization as a result of coercivity changes in rock samples from zones of hypergenesis, *Izv. Akad. Nauk SSSR, Fiz. Zemli*, 1987, no. 9, pp. 55–63.
- Brown, D. and Spadea, P., Processes of forearc and accretionary complex formation during arc–continent collision in the southern Ural Mountains, *Geology*, 1999, vol. 27, no. 7, pp. 649–652. [https://doi.org/10.1130/0091-7613\(1999\)027](https://doi.org/10.1130/0091-7613(1999)027)
- Brown, D., Alvarez-Marrón, J., Pérez-Estaún, A., Gorozhanina, Y., Baryshev, V., and Puchkov, V., Geometric and kinematic evolution of the foreland thrust and fold belt in the southern Urals, *Tectonics*, 1997, vol. 16, no. 3, pp. 551–562. <https://doi.org/10.1029/97tc00815>
- Brown, D., Juhlin, C., Alvarez-Marron, J., Pérez-Estaún, A., and Oslianski, A., Crustal-scale structure and evolution of an arc–continent collision zone in the southern Urals, Russia, *Tectonics*, 1998, vol. 17, no. 2, pp. 158–170. <https://doi.org/10.1029/98TC00129>
- Brown, D., Hetzel, R., and Scarrow, J.H., Tracking arc–continent collision subduction zone processes from high-pressure rocks in the Southern Urals, *J. Geol. Soc.*, 2000, vol. 157, no. 5, pp. 901–904. <https://doi.org/10.1144/jgs.157.5.901>
- Brown, D., Alvarez-Marrón, J., Pérez-Estaún, A., Puchkov, V., Gorozhanina, Y., and Ayarza, P., Structure and evolution of the Magnitogorsk forearc basin: Identifying upper crustal processes during arc–continent collision in the southern Urals, *Tectonics*, 2001, vol. 20, no. 3, pp. 364–375. <https://doi.org/10.1029/2001TC900002>
- Chadima, M. and Hroudá, F., Remasoft 3.0: A user-friendly paleomagnetic data browser and analyzer, *Travaux Géophysiques*, 2006, vol. 27, pp. 20–21.
- Danukalov, N.F., Komissarova, R.A., and Mikhailov, P.N., *Riphean stratotype, Paleontologiya. Paleomagnetizm (Paleontology. Paleomagnetism.)*, Keller, B.M., Ed., Moscow: Nauka, 1982, pp. 121–162.
- Debiche, M.G. and Watson, G.S., Confidence limits and bias correction for estimating angles between directions with applications to paleomagnetism, *J. Geophys. Res.: Solid Earth*, 1995, vol. 100, no. B12, pp. 24405–24429. <https://doi.org/10.1029/92jb01318>
- Doyle, K.A., Poulton, S.W., Newton, R.J., Podkovyrov, V.N., and Bekker, A., Shallow water anoxia in the Mesoproterozoic ocean: Evidence from the Bashkir Meganticlinorium, Southern Urals, *Precambrian Res.*, 2018, vol. 317, pp. 196–210. <https://doi.org/10.1016/j.precamres.2018.09.001>
- Dunlop, D.J., Thermal enhancement of magnetic susceptibility, *J. Geophys.*, 1974, vol. 40, no. 1, pp. 439–451. <https://doi.org/https://n2t.net/ark:/88439/y022154>
- Edel, J.B. and Schneider, J.L., The Late Carboniferous to Early Triassic geodynamic evolution of Variscan Europe in the light of magnetic overprints in Early Permian rhyolites from the northern Vosges (France) and central Black Forest (Germany), *Geophys. J. Int.*, 1995, vol. 122, no. 3, pp. 858–876. <https://doi.org/10.1111/j.1365-246x.1995.tb06842.x>
- Enkin, R.J., *A computer program package for analysis and presentation of paleomagnetic data*, Pacific Geoscience Centre, Geological Survey of Canada, 1994.
- Ernst, R.E., Pease, V., Puchkov, V.N., Kozlov, V.I., Sergeeva, N.D., and Hamilton, M., Geochemical characterization of precambrian magmatic suites of the southeastern margin of the East European Craton, Southern Urals, Russia, *Geol. Sb.*, 2006, no. 5, pp. 119–161. <https://www.elibrary.ru/vuybgh>.
- Ernst, R.E., Kheins, Dzh.A., Puchkov, V.N., Okrugin, A.V., and Archibal'd, D.A., Reconnaissance Ar–Ar dating of Proterozoic dolerite dykes and sills in Siberia and the Southern Urals: Identification of new major magmatic provinces and use in reconstruction of the Nuna supercontinent (Columbia), *Materialy Soveshchaniya MTK* (Proc. MTK Meeting), Moscow: GEOS, 2008, vol. 2, pp. 320–321.
- Evans, D.A.D. and Mitchell, R.N., Assembly and breakup of the core of Paleoproterozoic–Mesoproterozoic supercontinent Nuna, *Geology*, 2011, vol. 39, no. 5, pp. 443–446. <https://doi.org/10.1130/G31654.1>

- Fisher, R., Dispersion on a sphere, *Proc. R. Soc. A: Math., Phys. Eng. Sci.*, 1953, vol. 217, no. 1130, pp. 295–305. <https://doi.org/10.1098/rspa.1953.0064>
- Glasmacher, U.A., Puchkov, V.N., Reynolds, P., Alekseyev, A.A., Gorozhanin, V., Walter, R., and Taylor, K., $^{40}\text{Ar}/^{39}\text{Ar}$ thermochronology west of the Main Uralian fault, Southern Urals, Russia, *Geologische Rundschau*, 1999, vol. 87, no. 4, pp. 515–525. <https://doi.org/10.1007/s005310050228>
- Glasmacher, U.A., Matenaar, I., Bauer, W., and Puchkov, V.N., Diagenesis and incipient metamorphism in the western fold-and-thrust belt, SW Urals, Russia, *Int. J. Earth Sci.*, 2004, vol. 93, no. 3, pp. 361–383. <https://doi.org/10.1007/s00531-004-0386-7>
- Glodny, J., Bingen, B., Austrheim, H., Molina, J.F., and Rusin, A., Precise eclogitization ages deduced from Rb/Sr mineral systematics: The Maksyutov complex, Southern Urals, Russia, *Geochimica Cosmochim. Acta*, 2002, vol. 66, no. 7, pp. 1221–1235. [https://doi.org/10.1016/s0016-7037\(01\)00842-0](https://doi.org/10.1016/s0016-7037(01)00842-0)
- Golovanova, I.V., Danukalov, K.N., Kadyrov, A.F., Khidiyatov, M.M., Sal'manova, R.Yu., Shakurov, R.K., Levashova, N.M., and Bazhenov, M.L., Paleomagnetism of sedimentary strata and the origin of the structures in the western slope of South Urals, *Izv., Phys. Solid Earth*, 2017, vol. 53, no. 2, pp. 311–319. <https://doi.org/10.1134/s1069351317010050>
- Golovanova, I.V., Danukalov, K.N., and Sal'manova, R.Yu., Late paleozoic remagnetisation as an independent indicator of tectonic processes in the Southern Urals, *Geol. Vestn.*, 2022, no. 2, pp. 56–68. <https://doi.org/10.31084/2619-0087/2022-2-5>
- Gorozhanin, V.M., Gorozhanina, E.N., Zakirova, A.D., and Panova, N.P., Geochemistry and geochronology of the main volcanics of the Early Riphean Skaksha complex (Southern Urals), *Geol. Sb.*, 2008, no. 7, pp. 167–178. <https://www.elibrary.ru/bypmwj>
- Gorozhanin, V.M., Puchkov, V.N., Gorozhanina, E.N., Sergeeva, N.D., Romanyuk, T.V., and Kuznetsov, N.B., The Navysh graben-rift of the South Urals as a fragment of the Early Proterozoic aulacogen, *Dokl. Earth Sci.*, 2014, vol. 458, no. 1, pp. 1052–1057. <https://doi.org/10.1134/s1028334x1409013x>
- Halvorsen, E., Palaeomagnetism and the age of the younger diabases in the Ny-Hellesund areas, S. Norway, *Norsk Geol. Tidsskr.*, 1970, vol. 50, pp. 157–166.
- Halvorsen, E., Lewandowski, M., and Jeleńska, M., Palaeomagnetism of the Upper Carboniferous Strzegom and Karkonosze Granites and the Kudowa granitoid from the Sudet Mountains, Poland, *Phys. Earth Planet. Inter.*, 1989, vol. 55, nos. 1–2, pp. 54–64. [https://doi.org/10.1016/0031-9201\(89\)90233-1](https://doi.org/10.1016/0031-9201(89)90233-1)
- Hetzl, R., Echtler, H.P., Seifert, W., Schulte, B.A., and Ivanov, K.S., Subduction- and exhumation-related fabrics in the Paleozoic high-pressure–low-temperature Maksyutov Complex, Antingan area, southern Urals, Russia, *Geol. Soc. Am. Bull.*, 1998, vol. 110, no. 7, pp. 916–930. [https://doi.org/10.1130/0016-7606\(1998\)110<0916:saerfi>2.3.co;2](https://doi.org/10.1130/0016-7606(1998)110<0916:saerfi>2.3.co;2)
- Iosifidi, A.G., Mac Niocaill, C., Khramov, A.N., Dekkers, M.J., and Popov, V.V., Palaeogeographic implications of differential inclination shallowing in permo-carboniferous sediments from the Donets basin, Ukraine, *Tectonophysics*, 2010, vol. 490, nos. 3–4, pp. 229–240. <https://doi.org/10.1016/j.tecto.2010.05.017>
- Iosifidi, A.G., Mikhaylova, V.A., Sal'naya, N.V., and Khramov, A.N., Palaeomagnetism of sedimentary rocks of the South Uralian Asha series: New data, *Neftegazovaya Geol. Teoriya Prakt.*, 2012, vol. 7, no. 4, p. 6. <https://www.elibrary.ru/plhdgr>
- Holodnov, V.V., Fershtater, G.B., Shagalov, E.S., and Shardakova, G.Yu., Riphean magmatism and ore formation, preceding the disclosure of the Uralian Paleoocean (western slope of the Southern Urals), *Litosfera*, 2017, vol. 17, no. 2, pp. 5–26. <https://doi.org/10.24930/1681-9004-2017-2-005-026>
- Khotylev, A.O., Evolution of Late Precambrian magmatism in the northern part of the Bashkir meganticlinorium, *Cand. (Geol.) Dissertation*, Moscow: Lomonosov Moscow State University, 2018.
- Khotylev, A.O., Tevelev, A.V., Bychkova, Ya.V., Latyshev, A.V., and Anosova, M.B., Mezoproterozoic basite magmatism of the Bashkirian meganticlinorium (Southern Urals): Age constraints, petrological and geochemical features, *Geodyn. Tectonophysics*, 2020, vol. 11, no. 2, pp. 219–243. <https://doi.org/10.5800/gt-2020-11-2-0471>
- Kirschvink, J.L., The least-squares line and plane and the analysis of palaeomagnetic data, *Geophys. J. Int.*, 1980, vol. 62, no. 3, pp. 699–718. <https://doi.org/10.1111/j.1365-246X.1980.tb02601.x>
- Knyazev, Yu.G., Knyazeva, O.Yu., Snachev, V.I., Zhdanov, A.V., Karimov, T.R., Aidarov, E.M., Masagutov, R.Kh., and Arslanova, E.R., Ural series, page 40: Ufa: Explanatory note, *Gosudarstvennaya geologicheskaya karta Rossiiskoi Federatsii. Mashtab 1 : 1000000 (trei'e pokolenie)* (State Geological Map of the Russian Federation. Scale 1 : 1000000 (third generation)), Zhdanov, A.V., Ed., 2013.
- Komissarova, R.A., Study of the ancient magnetization of some sedimentary rocks of the Southern Urals in connection with the problem of metachronous remagnetization, *Cand. (Phys.-Math.) Dissertation*, Moscow: Schmidt Inst. of the Physics of the Earth, 1970.
- Konrad, H.J. and Nairn, A.E.M., The palaeomagnetism of the Permian rocks of the Black Forest, Germany, *Geophys. J. Int.*, 1972, vol. 27, no. 4, pp. 369–382. <https://doi.org/10.1111/j.1365-246x.1972.tb06098.x>
- Kovalev, S.G., Vysotskii, S., Puchkov, V.N., and Maslov, A.V., *Geokhimicheskaya spetsializatsiya strukturnoveshchestvennykh kompleksov Bashkirskogo megantiklinoriya*, Ufa: Dizain-Press, 2013.
- Kozlov, V.I., Makushin, A.A., and Shalaginov, V.V., *Geologicheskaya karta Rossiiskoi federatsii i sopredel'noi territorii Respubliki Kazakhstan N-40 (41) (Ufa). Novaya seriya. Karta dochetvertichnykh obrazovaniy, masshtab 1 : 100000* (Geological map of the Russian Federation and the adjacent territory of the Republic of Kazakhstan N-40 (41) (Ufa): New series. Map of prequaternary formations, scale 1 : 100000), Kozlov, V.I., Ed., St. Petersburg: Vseross. Geol. Inst., 2001.
- Krasnobaev, A.A., *Tsirkon kak indikator geologicheskikh protsessov* (Zircon As an Indicator of Geological Processes), Moscow: Nauka, 1986.
- Krasnobaev, A.A. and Borodina, N.S., *Geochemical peculiarities, genesis and age correlation of rifeic granitoids and liparite porphyries of the Zlatoust region (Southern Urals)*, Vo-

- prosy petrologii granitoidov Urala (Petrology of the Ural Granitoids)*, Sverdlovsk: Ural. Filial Akad. Nauk SSSR, 1970, pp. 124–153.
- Krasnobaev, A.A., Fershtater, G.B., Bea, F., and Montero, P., *Zircon age of gabbro and granitoids of the Kusinsk-Kopan complex (Southern Urals)*, *Ezhegodnik–2005 (Yearbook 2005)*, Ekaterinburg: Ural. Otd. Ross. Akad. Nauk, 2006, pp. 300–303.
- Krasnobaev, A.A., Puchkov, V.N., Kozlov, V.I., Sergeeva, N.D., Busharina, S.V., and Lepekhina, E.N., Zirconology of Navysk volcanic rocks of the Ai Suite and the problem of the age of the Lower Riphean boundary in the Southern Urals, *Dokl. Earth Sci.*, 2013, vol. 448, no. 2, pp. 185–190. <https://doi.org/10.1134/s1028334x13020050>
- Krs, M., Krsová, M., Kouklíková, L., Pruner, P., and Valín, F., On the applicability of oil shale to palaeomagnetic investigations, *Phys. Earth Planet. Inter.*, 1992, vol. 70, nos. 3–4, pp. 178–186. [https://doi.org/10.1016/0031-9201\(92\)90180-4](https://doi.org/10.1016/0031-9201(92)90180-4)
- Kurtukova, A.I., Ryazantsev, A.V., Golionko, B.G., and Travin, A.V., Wendian and Late Paleozoic plume-related gabbroic intrusions in the structure of the Bashkir megacyclinorium: New data on structural position and age (U–Pb SIMS, $^{39}\text{Ar}/^{40}\text{Ar}$), *Materialy Tektonicheskogo soveshchaniya (Proc. Tectonic Meeting)*, Moscow, 2022, vol. 1, pp. 254–258.
- Kuznetsov, A.B., Ovchinnikova, G.V., Semikhatov, M.A., Gorokhov, I.M., Kaurova, O.K., Krupenin, M.T., Vasil'eva, I.M., Gorokhovskii, B.M., and Maslov, A.V., The Sr isotopic characterization and Pb–Pb age of carbonate rocks from the Satka formation, the Lower Riphean Burzyan Group of the southern Urals, *Stratigr. Geol. Correl.*, 2008, vol. 16, no. 2, pp. 120–137. <https://doi.org/10.1134/s0869593808020020>
- Kuznetsov, A.B., Bekker, A., Ovchinnikova, G.V., Gorokhov, I.M., and Vasilyeva, I.M., Unradiogenic strontium and moderate-amplitude carbon isotope variations in early Tonian seawater after the assembly of Rodinia and before the Bitter Springs Excursion, *Precambrian Res.*, 2017, vol. 298, pp. 157–173. <https://doi.org/10.1016/j.precamres.2017.06.011>
- Latyshev, A.V., Anosova, M.B., and Khotylev, A.O., Paleomagnetism of the Early–Middle Riphean intrusions from the Bashkirian meganticlinorium (the Southern Urals): Implications for the paleotectonic reconstructions of the East European craton, *Geol. Vestn.*, 2019, no. 1, pp. 113–132. <https://doi.org/10.31084/2619-0087/2019-1-9>
- Levashova, N.M., Bazhenov, M.L., Meert, J.G., Kuznetsov, N.B., Golovanova, I.V., Danukalov, K.N., and Fedorova, N.M., Paleogeography of Baltica in the Ediacaran: Paleomagnetic and geochronological data from the clastic Zigan Formation, South Urals, *Precambrian Res.*, 2013, vol. 236, pp. 16–30. <https://doi.org/10.1016/j.precamres.2013.06.006>
- Maslov, A.V., Riphean and Vendian sedimentary sequences of the Timanides and Uralides, the eastern periphery of the East European Craton, *Geol. Soc., London, Memoirs*, 2004, vol. 30, no. 1, pp. 19–35. <https://doi.org/10.1144/gsl.mem.2004.030.01.03>
- Maslov, A.V., Erdtmann, B.-D., Ivanov, K.S., Ivanov, S.N., and Krupenin, M.T., The main tectonic events, depositional history, and the paleogeography of the southern Urals during the Riphean–early Palaeozoic, *Tectonophysics*, 1997, vol. 276, nos. 1–4, pp. 313–335. [https://doi.org/10.1016/s0040-1951\(97\)00064-4](https://doi.org/10.1016/s0040-1951(97)00064-4)
- Maslov, A.V., Gareev, E.Z., and Krupenin, M.T., *Osa-dochnye posledovatel'nosti rifeya tipovoi mestnosti (retrospektivnyi obzor sedimentologicheskikh, paleogeograficheskikh, litologo-mineralogicheskikh i petrogeokhimicheskikh issledovaniy)* (Riphean Sedimentary Sequences of Type Locality (Retrospective Review of Sedimentological, Paleogeographic, Lithologic–Mineralogical and Petrogeochemical Studies)), Ufa: GP Print, 1998.
- Maslov, A.V., Gareev, E.Z., and Kovalev, S.G., *Lithochemical peculiarities of terrigenous rocks of the Lower Riphean Ai Formation of the Bashkirian megazone: New data*, *Ezhegodnik-2012 (Yearbook 2012)*, Ekaterinburg: Inst. Geologii i Geokhimii Ural. Otd. Ross. Akad. Nauk, 2013, pp. 118–122.
- Matte, P., Maluski, H., Caby, R., Nicolas, A., Kepzhinskas, P., and Sobolev, S., Geodynamic model and $^{39}\text{Ar}/^{40}\text{Ar}$ dating for the generation and emplacement of the high pressure (HP) metamorphic rocks in SW Urals, *C. R. Acad. Sci., Ser. II*, 1993, vol. 317, pp. 1667–1674.
- Merabet, N. and Guillaume, A., Palaeomagnetism of the Permian rocks of Lodève (Hérault, France), *Tectonophysics*, 1988, vol. 145, nos. 1–2, pp. 21–29. [https://doi.org/10.1016/0040-1951\(88\)90312-5](https://doi.org/10.1016/0040-1951(88)90312-5)
- Nagata, T., *Rock Magnetism*, Tokyo: Maruzen, 1961.
- Nawrocki, J., Permian to Early Triassic magnetostratigraphy from the Central European Basin in Poland: Implications on regional and worldwide correlations, *Earth Planet. Sci. Lett.*, 1997, vol. 152, nos. 1–4, pp. 37–58. [https://doi.org/10.1016/s0012-821x\(97\)00147-7](https://doi.org/10.1016/s0012-821x(97)00147-7)
- Nawrocki, J., Fanning, M., Lewandowska, A., Polechońska, O., and Werner, T., Palaeomagnetism and the age of the Cracow volcanic rocks (S Poland), *Geophys. J. Int.*, 2008, vol. 174, no. 2, pp. 475–488. <https://doi.org/10.1111/j.1365-246x.2008.03804.x>
- Nosova, A.A., Sazonova, L.V., Kargin, A.V., Larionova, Yu.O., Gorozhanin, V.M., and Kovalev, S.G., Mesoproterozoic within-plate igneous province of the western urals: Main petrogenetic rock types and their origin, *Petrology*, 2012, vol. 20, no. 4, pp. 356–390. <https://doi.org/10.1134/s086959111204008x>
- Ovchinnikova, G.V., Kuznetsov, A.B., Vasil'eva, I.M., Gorokhov, I.M., Krupenin, M.T., Gorokhovskii, B.M., and Maslov, A.V., Pb–Pb age and Sr isotopic characteristic of the Middle Riphean phosphorite concretions: The Zigaza-Komarovo Formation of the South Urals, *Dokl. Earth Sci.*, 2013, vol. 451, no. 2, pp. 798–802. <https://doi.org/10.1134/s1028334x13080047>
- Parnachev, V.P., *Formation affiliation of the Riphean volcanogenic-sedimentary complexes of the Riphean of the Bashkir uplift, Dokembrii v fanerozoïskikh skladchatykh poyasakh (Precambrian in Phanerozoic Fold Belts)*, Leningrad: Nauka, 1982, pp. 96–106.
- Pavlov, V.E. and Gallet, Y., Katav limestones: A unique example of remagnetization or an ideal recorder of the neoproterozoic geomagnetic field, *Izv., Phys. Solid Earth*, 2009, vol. 45, no. 1, pp. 31–40. <https://doi.org/10.1134/S1069351309010054>
- Puchkov, V.N., *Paleogeodinamika Yuzhnogo i Srednego Urala (Paleogeodynamics of the Southern and Middle Urals)*, Ufa: Gilem, 2000.

- Puchkov, V.N., The evolution of the Uralian orogen, *Geol. Soc., London, Special Publ.*, 2009, vol. 327, no. 1, pp. 161–195.
<https://doi.org/10.1144/sp327.9>
- Puchkov, V.N., *Geologiya Urala i Priural'ya (aktual'nye vo-prosy stratigrafii, tektoniki, geodinamiki i metallogenii)* (Geology of the Urals and Cis-Urals (Actual Issues of Stratigraphy, Tectonics, Geodynamics and Metallogeny)), Ufa: DizainPoligrafServis, 2010.
- Puchkov, V.N., Kozlov, V.I., and Krasnobaev, A.A., Paleozoic U–Pb SHRIMP dating of igneous rocks of the Bashkir meganticlinorium, *Geol. Sb.*, 2011, no. 9, pp. 36–43.
<https://www.elibrary.ru/sywsyx>.
- Puchkov, V.N., Bogdanova, S.V., Ernst, R.E., Kozlov, V.I., Krasnobaev, A.A., Söderlund, U., Wingate, M.T.D., Postnikov, A.V., and Sergeeva, N.D., The ca. 1380Ma Mashak igneous event of the Southern Urals, *Lithos*, 2013, vol. 174, pp. 109–124.
<https://doi.org/10.1016/j.lithos.2012.08.021>
- Puchkov, V.N., Sergeeva, N.D., and Krasnobaev, A.A., Stratigraphic scheme of the Riphean stratotype of the Southern Urals, *Geol., Izv. Otdeleniya Nauk o Zemle Prirodnikh Resursov*, 2017, no. 23, pp. 3–26. <https://www.elibrary.ru/zspzrt>.
- Remaine, J., Cita, M.B., and Dercourt, J., *International Stratigraphic Chart and Explanatory Note*, IUGS-UNESCO, 2000.
- Ronkin, Yu.L., Tichomirowa, M., and Maslov, A.V., The Southern Urals Large Igneous Province with an age of approximately 1380 Ma: Precision U–Pb ID-TIMS constraints, *Dokl. Earth Sci.*, 2016, vol. 468, no. 2, pp. 587–592.
<https://doi.org/10.1134/s1028334x16060210>
- Rykus, M.V., Snachev, V.I., and Bazhin, E.A., Anorogenic granites of western slope of the Southern Urals: Composition, petrogenesis, mineralization, *Neftegaz. Delo*, 2011, no. 5, pp. 282–301. <https://www.elibrary.ru/pdwixn>.
- Salikhov, D.N. and Yarkova, A.V., *Nizhnkamennougol'nyi vulkanizm Magnitogorskogo megasinklinoriya* (Lower Carboniferous Volcanism of the Magnitogorsk Megasyntinorium), Ufa: Inst. Geologii Ufimskii Nauchnyi Tsentr Ross. Akad. Nauk, 1992, vol. 138.
- Semikhatov, M.A., Shurkin, K.A., Aksenov, Ye.M., Bekker, Yu.R., Bibikova, Ye.V., Duk, V.L., Yesipchuk, K.Ye., Karsakov, L.P., Kiselev, V.V., Kozlov, V.L., Lobach-Zhuchenko, S.B., Negrutsa, V.Z., Robonen, V.I., Sez'ko, A.I., Filatova, L.I., Khomentovskiy, V.V., Shemyakin, V.M., and Shul'diner, V.I., A new stratigraphic scale for the Precambrian of the USSR, *Int. Geol. Rev.*, 1991, vol. 33, no. 5, pp. 413–422.
<https://doi.org/10.1080/00206819109465699>
- Shatskij, V.S., Yagoutts, E., and Koz'menko, O.A., Sm–Nd-dating of high-pressure metamorphism of Maksyutov complex (Southern Urals), *Dokl. Akad. Nauk*, 1997, vol. 352, no. 6, pp. 812–815.
- Shcherbakov, V.P., Gribov, S.K., Lhuillier, F., Aphinogenova, N.A., and Tsel'movich, V.A., On the reliability of absolute palaeointensity determinations on basaltic rocks bearing a thermochemical remanence, *J. Geophys. Res.: Solid Earth*, 2019, vol. 124, no. 8, pp. 7616–7632.
<https://doi.org/10.1029/2019jb017873>
- Shipunov, S.V., Paleomagnetism of the Katav Formation, Southern Urals, *Izv.: Phys. Solid Earth*, 1991, vol. 27, p. 241.
- Shipunov, S.V., *Osnovy paleomagnitnogo analiza: Teoriya i praktika* (Fundamentals of Paleomagnetic Analysis: Theory and Practice), Trudy Geol. Inst. (Proc. Geol. Inst.), vol. 487, Moscow: Nauka, 1993.
- Shipunov, S.V., Synfold magnetization: Estimation of its direction and geological implications, *Izv., Phys. Solid Earth*, 1995, vol. 31, pp. 948–955.
- Shipunov, S.V., Folding history of the Southern Urals according to paleomagnetic data, *Paleomagnetizm i magnetizm gornyx porod*, Moscow: Ob'edinennyi Inst. Fiz. Zemli Ross. Akad. Nauk, 1998, pp. 69–71.
- Smith, R.L. and Piper, J.D.A., Palaeomagnetism of the Särna alkaline body, *Geologiska Föreningen Stockholm Förhandlingar*, 1979, vol. 101, no. 2, pp. 167–168.
<https://doi.org/10.1080/11035897909452576>
- Stratotip rifeya. Stratigrafiya. Geokhronologiya (Riphean Stratotype. Stratigraphy. Geochronology)*, Keller, B.M., Ed., Moscow: Nauka, 1983.
- Sturt, B.A. and Torsvik, T.H., A late Carboniferous palaeomagnetic pole recorded from a syenite still, Stabben, Central Norway, *Phys. Earth Planet. Inter.*, 1987, vol. 49, nos. 3–4, pp. 350–359.
[https://doi.org/10.1016/0031-9201\(87\)90036-7](https://doi.org/10.1016/0031-9201(87)90036-7)
- Svyazhina, I.A., Puchkov, V.N., Ivanov, K.S., and Petrov, G.A., *Paleomagnetizm Urala* (Paleomagnetism of the Urals), Ekaterinburg: Inst. Geologii Ural. Otd. Ross. Akad. Nauk, 2003.
- Thomas, D.N., Rolph, T.C., and Friel, D.F., Permo-Carboniferous (Kiaman) palaeointensity results from the western Bohemian Massif, Germany, *Geophys. J. Int.*, 1997, vol. 130, no. 1, pp. 257–265.
<https://doi.org/10.1111/j.1365-246x.1997.tb01004.x>
- Torsvik, T.H., Van Der Voo, R., Preeden, U., Mac Niocaill, C., Steinberger, B., Doubrovine, P.V., Van Hinsbergen, D.J.J., Domeier, M., Gaina, C., Tohver, E., Meert, J.G., Mccausland, P.J.A., and Cocks, L.R.M., Phanerozoic polar wander, palaeogeography and dynamics, *Earth-Sci. Rev.*, 2012, vol. 114, nos. 3–4, pp. 325–368.
<https://doi.org/10.1016/j.earscirev.2012.06.007>
- Vinogradov, E.V., Paleomagnetism of Ordovician–Silurian sediments of the West Zilairian zone of the Southern Urals, *Materialy mezhdunarodnoi shkoly-seminara Problemy paleomagnetizma i magnetizma gornyx porod* (Proceedings of the International School-Seminar Problems of Paleomagnetism and Magnetism of Rocks), Yaroslavl: Filigran', 2016, pp. 18–23.
- Yuan, K., Van der Voo, R., Bazhenov, M.L., Bakhmutov, V., Alekhin, V., and Hendriks, B.W.H., Permian and Triassic palaeolatitudes of the Ukrainian shield with implications for Pangea reconstructions, *Geophys. J. Int.*, 2010, vol. 184, no. 2, pp. 595–610.
<https://doi.org/10.1111/j.1365-246x.2010.04889.x>

Translated by A. Ivanov

Publisher's Note. Pleiades Publishing remains neutral with regard to jurisdictional claims in published maps and institutional affiliations.